Lanthipeptide engineering: non-canonical amino acids, click chemistry and ring shuffling

Deng, Jingjing

DOI:
10.33612/diss.112973724

CHAPTER 3

Analysis of modular bioengineered antimicrobial lanthipeptides at nanoliter scale

Steven Schmitt[1†], Manuel Montalbán-López[2†], David Peterhoff[3], Jingjing Deng[2], Ralf Wagner[3,4], Martin Held[1], Oscar P. Kuipers[2], and Sven Panke[1]

[1] ETH Zürich, Department of Biosystems Science and Engineering, Basel, Switzerland
[2] University of Groningen, Department of Molecular Genetics, Groningen, The Netherlands.
[3] University of Regensburg, Institute of Medical Microbiology and Hygiene, Regensburg, Germany.
[4] University Hospital Regensburg, Institute of Clinical Microbiology and Hygiene, Regensburg, Germany.
[†] These authors contributed equally to this work.

Published in: *Nature chemical biology* **15**, 437-443, doi: 10.1038/s41589-019-0250-5 (2019).

I contributed to the purification and determination of the MICs of the peptides and to parts of the writing.

Abstract

The rise of antibiotic resistances demands the acceleration of molecular diversification strategies to inspire new chemical entities for antibiotic medicines. We report here on the large-scale engineering of ribosomally synthesized and post-translationally modified antimicrobial peptides carrying the ring-forming amino acid lanthionine. New-to-nature variants featuring distinct properties were obtained by combinatorial shuffling of peptide modules derived from 12 natural antimicrobial lanthipeptides and processing by a promiscuous post-translational modification machinery. For experimental characterization, we developed the nanoFleming, a miniaturized and parallelized high-throughput inhibition assay. Based on a hit set of >100 molecules, we identified variants with improved activity against pathogenic bacteria and shifted activity profiles, and extrapolated design guidelines which will simplify the identification of peptide-based anti-infectives in the future.

Introduction

Close to 75% of all approved antibiotics have their origin in nature, highlighting the importance of natural products for drug development[1]. However, identifying new lead molecules from this pool, preferably with novel modes of action, is becoming increasingly difficult[2–5]. The further development of existing molecules by chemical diversification, another well-established strategy[6], delivers only limited structural novelty. More recently, biological diversification of enzymatically produced natural products (such as non-ribosomal peptides or polyketides) has been introduced. This strategy relies on the recombination of the involved enzyme clusters and delivered promising leads[7,8]. However, the lack of insight into how to generate sufficient modularity for efficient enzyme shuffling and the restricted experimental throughput to explore large combinatorial spaces limit the impact on drug development[9,10].

In practical terms, molecule diversification in bioengineering approaches becomes much easier if the antimicrobial molecule is a gene product itself rather than the catalytic result of several gene products whose engineering has to be carefully coordinated. One such example of a gene-encoded natural product are ribosomally produced and post-translationally modified peptides (RiPPs)[11]. Here, application of the well-developed methods of DNA synthesis and modification allow direct synthesis of highly diverse peptides, which are then further modified with the functionally important post-translational modification machinery. Among RiPPs, the class of antimicrobial lanthipeptides (i.e. lantibiotics) represents a rich source for promising leads against Gram-positive bacteria. The best-known representative, nisin, already has as a long history as a food preservation agent and others entered recently into clinical development for infectious diseases[12,13]. Lantibiotics carry ring-forming amino acids (lanthionine and methyllanthionine) that result in small peptide stretches that are considerably restricted in their rotational degree of freedom (Figure 1a) and are introduced by an, often promiscuous, post-translational modification (PTM) machinery (Supplementary Figure 1), suggesting the possibility for diversifying the peptide backbone, while still enabling modifications[14–19].

Lantibiotics commonly bind to the bacterial cell wall precursor lipid II, inhibiting cell wall formation and often also induce pore formation in the cytoplasmic membrane of their target cells[20]. They feature a similar blueprint encompassing the location of functional elements (lipid II binding and membrane piercing) as well as the organization of the thioether rings within the peptide backbone (Figure 1a). However, the ring structures themselves vary considerably in size and primary structure over different peptides and the peptides display highly different degrees of activity towards target strains[20]. This diversity raises the intriguing opportunity of large-scale molecular shuffling to obtain novel functionality based on modules broadly organized along

ring structures and other functional segments (Figure 1b). In order to overcome the otherwise prohibitive issue of sorting through large numbers of peptide variants, we miniaturized Fleming's inhibition zone assay[21] by evaluating the result of coculturing RiPP producers and a sensor strain at nanoliter scale ("nanoFleming") in nanoliter reactors (nLRs) and at high-throughput[22–25]. Here we present the results of shuffling 33 lantibiotic peptide modules with natural or synthetic background yielding a library of 6,000 putatively active structures. Screening of the library with the nanoFleming platform followed by detailed characterization resulted in a set of 11 antimicrobial lanthipeptides that showed improved antimicrobial activity over wild-type peptides or were able to bypass resistance mechanisms.

Results

Design of a combinatorial lanthipeptide library

Peptide modules were recruited from twelve natural lantibiotics (Supplementary Table 1) representing broadly linear peptides with lipid II binding and pore formation (type A lantibiotics, including nisin), globular peptides with large and intertwined rings with lipid II affinity, but without perforation capacity (type B lantibiotics, e.g. actagardine), and peptides with a lipid II binding and a pore-forming subunit (two-component lantibiotics, e.g. haloduracin). The peptides were modularized according to rotationally restricted regions comprised of one single or two interwoven thioether rings and flexible, interconnecting ("hinge") regions. For nisin, we identified five modules (binding modules B1 and B2 involved in lipid II binding and pore modules P1 to P3 involved in pore formation, Figure 1a), extracted a further 23 modules from the remaining 11 lantibiotics, and allocated those to positions B1 to P3 (Figure 1b). The set was completed with non-natural interconnecting hinge modules (P2) of different lengths and charges to increase the likelihood for activities against different target strains[26] and a placeholder at P1 to represent natural lantibiotics missing this module (e.g. gallidermin). Finally, we limited B1 to modules from nisin and gallidermin as this module is critical for PTM by the nisin biosynthetic machinery (*vide infra*)[17]. Next, we generated new-to-nature peptides by randomly combining one module of each of the five groups, employing chemical synthesis of the peptide-encoding DNA and a split-and-mix approach to implement modular recombination (Supplementary Figure 2). PTM and export of lantibiotics are dependent on an N-terminal leader peptide; therefore the resulting DNA library of 6,000 combinatorial variants was fused to the leader peptide of nisin and overexpressed in a *Lactococcus lactis* also expressing the nisin PTM machinery NisBTC (i.e. including the nisin export function NisT but excluding the protease NisP required for peptide activation by cleavage of the leader peptide)[19] (Figure 1c).

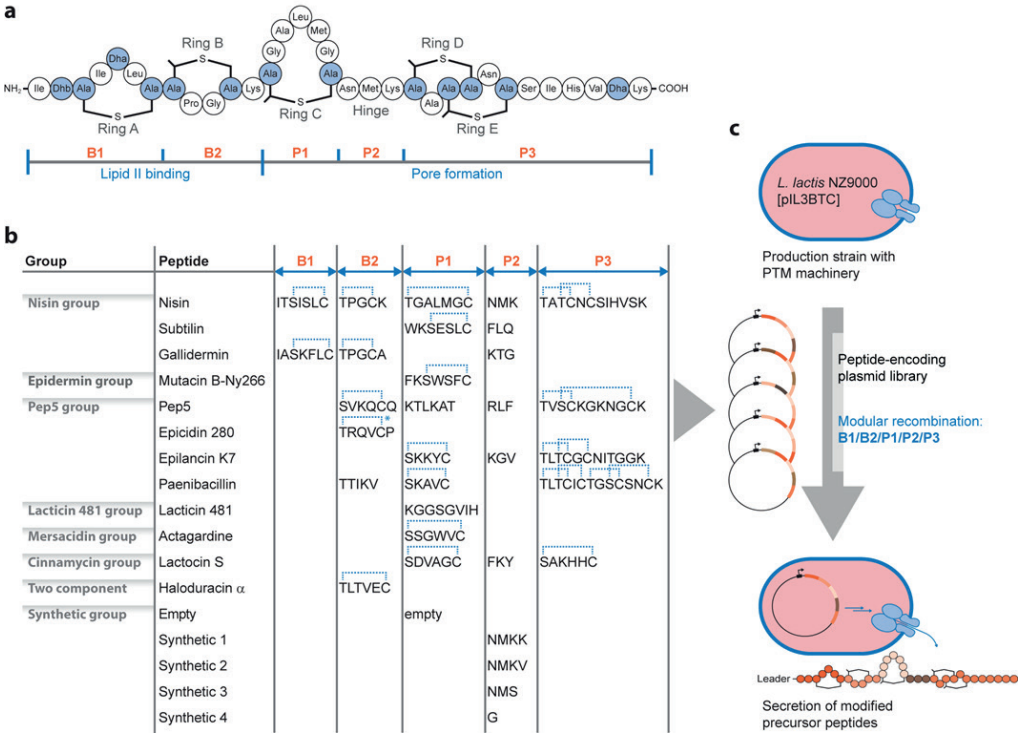

Figure 1. Modular assembly of antimicrobial lanthipeptides. (**a**) Module-reflecting blueprint of the lantibiotic nisin with the thioether rings A to E and the hinge region translated into five peptide modules B1 to P3. (**b**) Segmentation and assignment of 12 natural lantibiotics into modules. Known (*=estimated) thioether rings are indicated. A fictitious P1 module (marked as "empty") is used in our design to mimic shorter lantibiotics (e.g. epidermin and gallidermin) that lack a sequence connecting B2 to the P2 region. (**c**) The different modules were shuffled by DNA synthesis retaining the sequence B1/B2/P1/P2/P3 and the library of 6,000 variants was overexpressed in the PTM-competent secretion host *L. lactis* NZ9000 [pIL3BTC].

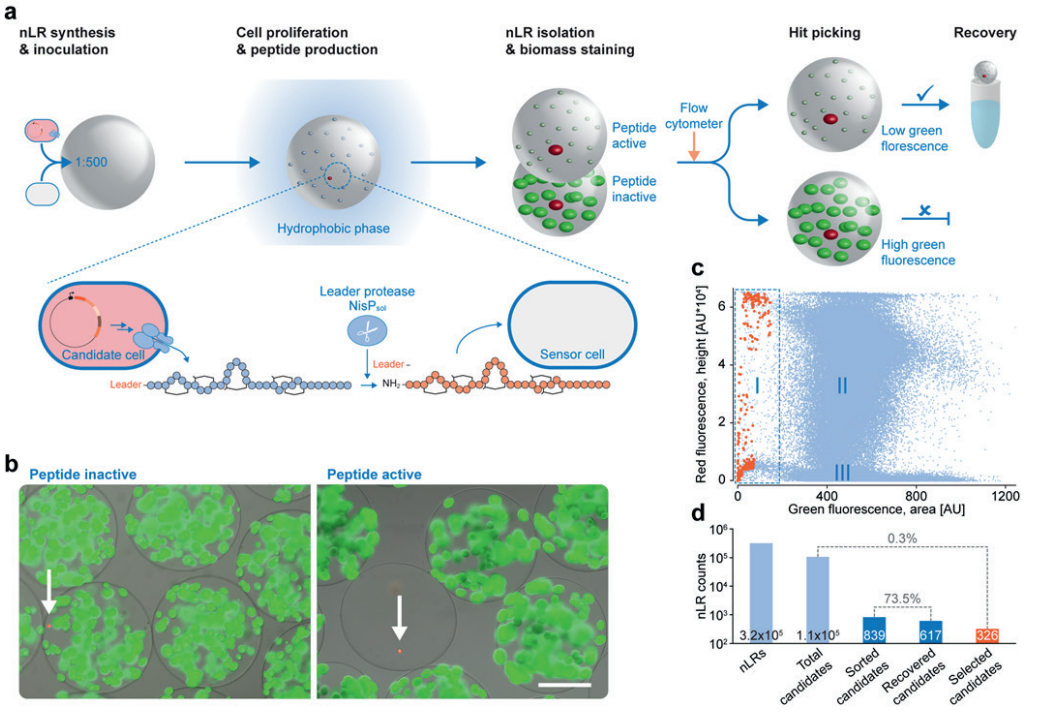

Figure 2. Discovery platform for antimicrobial peptides. (**a**) nanoFleming workflow: Library (peptide secreting and a red fluorescent protein mCherry producing *L. lactis*, in red) and sensor (*M. flavus*) cells are encapsulated in nLRs at 0.3 and 150 cells nLR^{-1}, respectively. Next, nLRs are soaked with growth medium containing the leader-specific protease NisPsol, resuspended in a hydrophobic phase, and incubated. Depending on the specific activity of the secreted peptides, the colocalized sensor cells may either continue to grow or experience different degrees of growth inhibition. After incubation, nLRs are recovered from the hydrophobic phase, stained and sorted based on the amount of sensor strain per nLR. Candidate cells in nLRs with little sensor biomass are recovered. (**b**) Overlay of bright-field and epifluorescence microscopic images of nLRs after incubation. Left: candidate colony (red, arrow) not secreting an active lantibiotic results in large sensor colonies (green). Right: candidate colony secreting an active lantibiotic (here: nisin). Scale bars: 200 µm. (**c**) Dot plot of the results from flow cytometric analysis of nLRs. 3.2×10^5 nLRs (blue dots) inoculated with 1.1×10^5 candidate cells (18-fold oversampling of the library). Red fluorescence indicated the size of the microcolony of candidate cells (region I+II = large; region III = small/absent) and green fluorescence indicated biomass of sensor cells (region I = low; region II+III = high). (**d**) Summary of isolated peptide candidates over the nanoFleming workflow.

Development of an inhibition assay at nanoliter scale

To enable rapid bioactivity assessment of the library peptides, we developed the nanoFleming high-throughput platform for antibiotic screening. We used small alginate hydrogel compartments (500 µm diameter, volume 65 nL, hence nLRs) for bacterial growth, peptide production and bioactivity testing. In a typical experiment, on average 0.3 library cells were encapsulated per nLR together with 150 cells of the sensor strain *Micrococcus flavus*. The nLRs were soaked in growth medium containing the soluble form of the protease NisP (NisPsol)[27] required for the activation of secreted peptides (Supplementary Figure 3). Incubation, conducted in a hydrophobic phase to prevent cross-talk between nLRs, allowed for the growth of library and sensor cells and peptide production. After incubation and recovery from the hydrophobic phase, the nLR-embedded biomass was stained with the fluorescent dye SYTO 9 and nLRs with no or only very little biomass, indicating effective prevention of sensor strain growth, were isolated (Figure 2a and Supplementary Figure 4). To characterize the assay, we first compared the inhibition of nLR-embedded sensors in the presence and absence of colocalized prenisin-secreting cells and found that candidate strains secreting prenisin, but not a non-secreting control strain, efficiently inhibited the growth of the sensors (Figure 2b and Supplementary Figure 5). We also observed a higher sensitivity of the nanoFleming assay when compared to standard inhibition zone assays (Supplementary Figure 6). This corroborated the suitability of the miniaturized assay for the identification of compounds in screening campaigns where production levels of the active substance might frequently be low.

Library screening and hit verification

Next, we screened the combinatorial peptide library using the nanoFleming platform (Figure 2c). Out of 3.2×10^5 nLRs, we isolated 839 nLRs (0.8%) containing very low levels of sensor biomass. The nLRs were spotted on agar plates and 617 of the embedded candidate strains (73.5%) could be regrown. We selected the 326 candidates that had shown the lowest green fluorescence in the screen for further processing.

The peptide-encoding DNA sequences of all isolated clones were determined and 205 unique peptide variants were characterized with respect to production level and antimicrobial activity. Each clone was grown in liquid culture, the secreted peptide was precipitated and the leader was fully cleaved with NisPsol. As only the sequence of the putatively antimicrobial core peptides but not the leader sequence varied, the production level and the fraction of correctly cleaved peptide could be estimated on the basis of the leader concentration by HPLCMSMS. Next, the activity of the mixture was analyzed with a conventional inhibition zone assay[28] against *M. flavus* (Supplementary Figure 7) and a panel of model pathogens (Supplementary Figure 8). The activity data as well as the production levels were compared to nisin as reference. From the group of

205 isolated clones, we identified 126 peptides that showed reproducible halo formation against *M. flavus*. Based on the DNA sequence data, heavily (modules from up to five different parents combined in a single peptide) as well as mildly shuffled antimicrobial peptides had been generated.

Design guidelines for bioactive lanthipeptides

We next set out to identify guidelines for the design of bioactive molecules based on the activity and secretion level of the 205 unique peptides obtained in the initial screen (126 positive, 79 negative). In order to ensure NisP cleavage, only two modules had been included for permutation at B1. Both were found in the screening hits and the corresponding peptides displayed considerable activity and production levels (Figure 3). At B2, the modules derived from gallidermin and nisin were clearly overrepresented in the fraction of the isolated peptides and seemed to facilitate processing and secretion as compared to the remaining 4 options. Furthermore, all peptides bearing these two modules had a rather high activity, possibly indicating efficient processing of the peptide by the NisBTC PTM machinery[17]. At P1, the structural variety found within the subset of efficiently produced peptides was much larger than at B2 and modules derived from actagardine, nisin, paenibacillin, pep5 and subtilin were found. Similarly, modules from actagardine, nisin and paenibacillin were found in active bacterial variants. For P2 (hinge region), all modules showed production (at variable mean levels) and were represented among bioactive peptides. Similar results were observed for P3: All 5 possible modules were among the population of analyzed peptides, but we again observed a clear overrepresentation of the nisin-derived module. Still, all modules tested for P3 were included in bioactive peptides. Taken together, 22 of the 33 modules that had been shuffled were afterwards identified in newly generated bioactive peptides. These results indicate that antimicrobial lanthipeptides can be assembled by combinatorial recombination of peptide modules and that despite a considerable variation of the amino acid sequence, most of these modules can become part of novel and bioactive peptides.

Minimal inhibitory concentrations against pathogens

Based on their activity in the preliminary assays and their modular diversity, we selected 61 peptides for further characterization. To facilitate the purification of the peptides in large quantities, we integrated a His_6-tag into the leader peptide. Modified precursor peptides were then purified via immobilized metal ion affinity chromatography (IMAC), the leader peptide was removed and the core peptides were further purified by RP-HPLC. For 31 peptides, this pipeline allowed purification of sufficient material to determine the minimal inhibitory concentration (MIC) against *M. flavus* and a panel of seven Gram-positive pathogenic strains, including *Streptococcus pneumoniae*, two

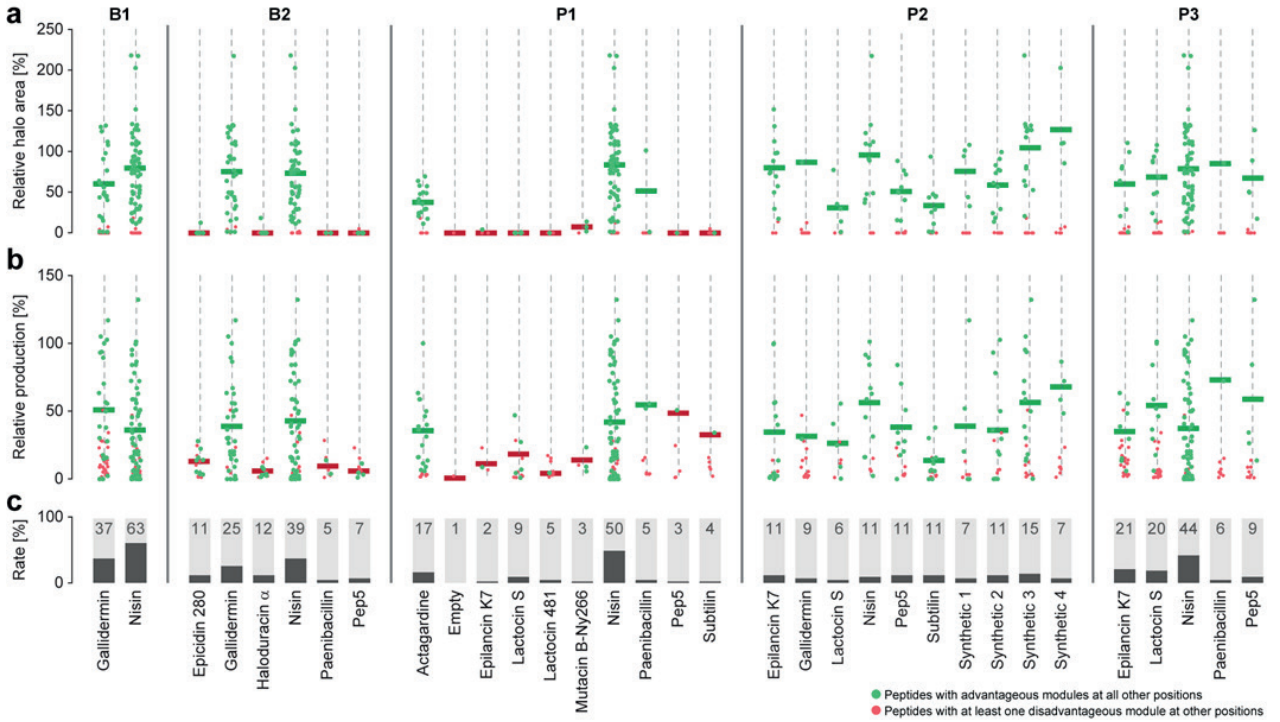

Figure 3. Characterization of screening hits. (**a**) Relative antimicrobial activity as a function of module nature and position. Each dot represents a peptide that was tested and had the specific module present in that position. Vertical bars: Mean of activities of all tested peptides with this module. Bar color indicates classification as advantageous (green, leading to a bioactive molecule) or disadvantageous (red, not leading to a bioactive molecule) module. Mean values were calculated from only those peptides which had advantageous modules at all other positions (green dots). (**b**) As in (a), but for relative production level. (**c**) Fraction of the module in all isolated variants (n = 205). All peptides were precipitated in duplicate (n = 2) and antimicrobial activity and production levels were quantified in triplicate. Each dot represents the mean of those measurements.

Table 1. MICs (μg mL^{1}) of combinatorial peptides against pathogens.

MIC [μg mL^{1}]	Module combination					*S. pneumoniae* TIGR-4	*S. pneumoniae* D39	*S. aureus* CAL (MRSA)	*S. aureus* MW2 (MRSA)	*E. faecalis* LMG 16216 (VRE)	*E. faecium* LMG 16003 (VRE)	*B. cereus* ATCC 14579
Peptide	B1	B2	P1	P2	P3							
1 SC5.2712	Gallidermin	Gallidermin	Nisin	Nisin	Nisin	0.53	0.42	7.36	38.90	7.36	7.36	37.85
2 SC5.1421	Gallidermin	Gallidermin	Nisin	Syn.1	Nisin	2.01	2.29	3.73	2.80	1.40	11.20	44.80
3 SC5.2930	Gallidermin	Nisin	Nisin	Syn.3	Nisin	0.84	1.13	26.97	17.98	290.0	6.74	26.97
Gallidermin						0.90	1.81	11.30	13.56	27.12	54.25	37.29
Nisin						4.21	4.21	9.86	10.91	6.68	7.72	12.19

MICs of a selected set of combinatorial peptides against a panel of seven Gram-positive model pathogens. Values that are improved in comparison to one of the wild-type peptides nisin or gallidermin are highlighted in grey. Values are means of three MIC experiments (n = 3).

methicillin resistant *Staphylococcus aureus*, vancomycin resistant *Enterococcus faecalis*, vancomycin resistant *E. faecium* and *Bacillus cereus*.

We observed a large MIC-range of the purified peptides against the screening strain *M. flavus*, with many of the peptides exhibiting an MIC of <0.5 μg mL^{-1} (Supplementary Table 2 and Supplementary Figure 9). Furthermore, we identified peptides with improved activity against one or more of the pathogenic reference strains when compared to nisin and gallidermin (Table 1). Nisin seems particularly active against both Enterococci and both Staphylococci strains and gallidermin against the two Streptococci strains. When combining the lipid II binding moiety B1 and B2 of gallidermin with the pore-forming modules P1-P3 of nisin, the combinatorial peptide 1 showed improved activities against Streptococci when compared to nisin and improved activities against one of the two Staphylococci and the two Enterococci when compared to gallidermin. The similar variant peptide 2 with an additional module exchange in P2 showed even better activity against the two Staphylococci and one Enterococci. Certain module combinations also led to peptides with strongly reduced activities against a specific strain, but retained a high specific activity against others, suggesting a possible increase in selectivity. For example, peptide 3 displayed good bioactivity against most strains of the test panel but activity against one of the Enterococci was strongly reduced when compared to nisin or gallidermin (Table 1).

Bypassing lantibiotic resistance mechanisms

Two specific microbial defense mechanisms against nisin are characterized[29]. One is constituted by the nisin immunity machinery, which is present in nisin-producing

Table 2. MICs (μg mL^{1}) of combinatorial peptides against nisin resistant strains.

a									
MIC [μg mL^{1}]		Module combination					*L. lactis*	*L. lactis*	
Peptide		B1	B2	P1	P2	P3	NZ9000	NZ9803	Immunity
1	SC5.2712	Gallidermin	Gallidermin	Nisin	Nisin	Nisin	0.05	1.30	25
3	SC5.2930	Gallidermin	Nisin	Nisin	Syn.3	Nisin	0.12	1.90	15
4	SC5.1659	Nisin	Nisin	Nisin	Syn.2	Nisin	0.80	12.00	14
5	SC5.1536	Nisin	Nisin	Nisin	Syn.4	Nisin	0.13	3.60	27
6	SC5.0925	Nisin	Gallidermin	Nisin	Syn.3	Nisin	0.03	4.00	132
Nisin							0.03	30.90	1029

b									
MIC [μg mL^{1}]		Module combination					*L. lactis* NZ9000	*L. lactis* NZ9000	
Peptide		B1	B2	P1	P2	P3	[pEmpty]	[pNSR]	Resistance
7	SC5.0718	Nisin	Nisin	Nisin	Pep 5	Lactocin S	0.65	0.65	0
8	SC5.2096	Nisin	Nisin	Nisin	Nisin	Pep 5	0.73	0.73	0
9	SC5.0364	Nisin	Nisin	Nisin	Syn.3	Pep 5	2.15	2.15	0
10	SC5.2354	Nisin	Nisin	Nisin	Syn.4	Paenibacillin	6.90	6.90	0
11	SC5.0479	Nisin	Nisin	Nisin	Syn.2	Epilancin K7	0.86	1.73	1
Nisin							0.08	1.63	19

*(**a**) MICs of a selected set of nisin-alike combinatorial peptides against a strain carrying the nisin immunity cluster on the genome (L. lactis NZ9803) and comparison to a strain that does not carry the cluster (L. lactis NZ9000). (**b**) MICs of a selected set of combinatorial peptides with various C-termini against a strain over-expressing the nisin resistance protein from a plasmid (NZ9000 [pNSR]) and comparison to a strain that carries an empty plasmid (NZ9000 [pEmpty]). Immunity and resistance are given as relative change (x/y-1). Values are means of three MIC experiments (n = 3).*

strains. This is composed of the proteins NisI and NisFEG, which prevent nisin binding to lipid II. The second mechanism is the nisin resistance protein (NSR) present in non-producing (pathogenic) strains. NSR works as a peptidase that cleaves the linear C-terminus of nisin (last 6 amino acids) after the interwoven rings DE and increases the MIC 20-fold. In the latter case, ring E is crucial for recognition[29,30]. We have identified both, peptides for which the natural nisin immunity system showed only reduced effectiveness by testing *L. lactis* NZ9803 expressing NisI and NisFEG (Table 2a) and for which a natural resistance determinant, the NSR from *S. agalactiae*, heterologously expressed by *L. lactis* NZ9000 [pNSR], no longer showed any activity (Table 2b).

Inference of structural features

Next to the bioactivity of those combinatorial peptides we were interested in the degree of post-translational modification introduced by NisB and NisC. We therefore analyzed

the final set of 11 peptides with improved activity against the pathogenic reference strains (Table 1) and the ability to bypass defense mechanisms (Table 2) by mass spectrometry. As the major modification pattern for all peptides analyzed we could identify a degree of dehydration of serine and threonine residues that is in the range of nisin (70 to 100%, nisin: 89%) and observed that except for peptide 7 (3 of 4) and peptide 10 (4 of 7) all cysteines were involved in thioether ring formation (Supplementary Figs. 10 and 11) and confirmed the success of the combinatorial design of novel lanthipeptides.

Discussion

Large-scale engineering of natural products is a promising strategy to obtain improved bioactive molecules but is suffering from two bottlenecks: a lack of insight into the determinants of functional modularity in large enzyme clusters and a lack of efficient methods to explore the antimicrobial activity of large sets of variants at high speed. Here, we show that assays for antimicrobial activity can be efficiently downscaled and parallelized, making the latter bottleneck obsolete. By switching from natural products whose structure is encoded in the reaction specificity of enzymes to those that are gene-encoded, such as lantibiotics, we drastically facilitate the production of potentially active molecule variants. We do not entirely escape the boundaries of enzyme specificity with this approach, as enzyme-based PTMs remain important, but the availability of promiscuous PTM systems as well as the sheer number of variants that DNA-manipulation can deliver in screens of the type demonstrated here, make the successful isolation of novel active, peptide-based natural products much more likely. We illustrate this by modular shuffling of lantibiotics, for which we could easily isolate 126 novel active antimicrobial peptides combining modules from other lantibiotics or of synthetic nature and some of them displaying improved or shifted activity profiles.

The presented strategy is scalable without adaptation of the protocol by increasing the number of modules, and it can readily be adapted to other pathogenic hosts[31] as well as to other library generation methods. In this study we focused on lipid II binding peptides and the nisin modification machinery. However, the strategy is applicable to all antimicrobial peptides as long as they are secreted by the producing host. We envision that the use of more diverse peptide modules, including those exhibiting a different mode-of-action, will enhance the diversity of the isolated bioactive peptides.

A bottleneck that cannot be entirely excluded is the substrate specificity of the PTM enzymes that limit the diversity of peptides that can be produced. However, given the capacity of the nanoFleming assay, future approaches might include various different PTM enzymes co-expressed in the production host or even include direct evolution on such enzyme to broaden their substrate specificity and therefore widen the diversity of the isolated antimicrobial peptides. When retaining the module shuffling strategy,

the length of the antimicrobial peptides in the library is currently restricted by the capabilities of chemical DNA synthesis (approx. 150 bases), which is sufficient for many RiPP genes, but can be extended using oligo-synthesis together with established assembly-strategies[32]. Also, the nanoFleming assay can be easily scaled to up to 10^6 clones per day, which is the current limit for large particle flow cytometry. In summary, the presented platform represents a powerful novel approach to the generation of topologically novel antimicrobial peptides.

In the future, this platform might not only be useful for the discovery of molecules with improved or altered bioactivity profiles but also for the generation of sufficient diversity required at other steps in drug development of peptides (e.g. to test candidate peptides for plasma stability or activity *in vivo*). Last, we envision the nanoFleming platform of help also for addressing other questions in peptide development, such as for the improvement of peptide secretion from host strains by genetic engineering.

Acknowledgements

We thank A. van de Vries (Department of Biosystems Science and Engineering (DBSSE), ETH Zürich) for assistance in protocol development, R. Pellaux, A. Meyer (both FGen GmbH), Tania Roberts (DBSSE) and A.J. van Heel (Department of Molecular Genetics, University of Groningen) for their valuable suggestions during the whole project. We thank the Genomics Facility Basel (C. Beisel, K. Eschbach, E.V. Burcklen, I. Nissen-Naidanow and M. Kohler, DBSSE) for their help with next generation sequencing and S. Posada-Céspedes (DBSSE) for her help with sequence analysis. Furthermore, the authors would like to thank A. Femmer (DBSSE) for her excellent technical assistance during peptide characterization and thank S. Smits for the pNSR construct. Last, S.S., M.M.-L., D.P., R.W., O.P.K. and S.P. would like to acknowledge funding from the ESF EUROCORES project "SYNMOD" (grant number FP-017) and the EU FP7 project "SYNPEPTIDE" (grant number 613981) and J.D. funding from the Chinese Scholarship Council (CSC).

References

1. Newman, D. J. & Cragg, G. M. Natural products as sources of new drugs from 1981 to 2014. *Journal of nature products* **79**, 629-661, doi:10.1021/acs.jnatprod.5b01055 (2016).
2. Zengler, K., Toledo, G., Rappe, M., Elkins, J., Mathur, E. J., Short, J. M. & Keller, M. Cultivating the uncultured. *Proceeding of the national academy of sciences* **99**, 15681-15686, doi:10.1073/pnas.252630999 (2002).
3. Baltz, R. H. Marcel faber roundtable: is our antibiotic pipeline unproductive because of starvation, constipation or lack of inspiration? *Journal of industrial microbiology and biotechnology* **33**, 507–513, doi:10.1007/s10295-005-0077-9 (2006).
4. Nichols, D., Cahoon, N., Trakhtenberg, E. M., Pham, L., Mehta, A., Belanger, A., Kanigan, T., Lewis, K. & Epstein, S. S. Use of iChip for high-throughput in situ cultivation of 'uncultivable' microbial species. *Applied and environmental microbiology* **76**, 2445-2450, doi:10.1128/AEM.01754-09 (2010).

5. Ling, L. L. et al. A new antibiotic kills pathogens without detectable resistance. *Nature* **517**, 455-459, doi:10.1038/nature14098 (2015).
6. Fischbach, M. A. & Walsh, C. T. Antibiotics for emerging pathogens. *Science* **325**, 1089-1093, doi:10.1126/science.1176667 (2009).
7. Walsh, C. T. Insights into the chemical logic and enzymatic machinery of NRPS assembly lines. *Nature product reports* **33**, 127-135, doi:10.1039/c5np000035a (2016).
8. Menzella, H. G., Reid, R., Carney, J. R., Chandran, S. S., Reisinger, S. J., Patel, K. G., Hopwood, D. A. & Santi, D. V. Combinatorial polyketide biosynthesis by *de novo* design and rearrangement of modular polyketide synthase genes. *Nature biotechnology* **23**, 1171-1176, doi:10.1038/nbt1128 (2005).
9. Winn, M., Fyans, J. K., Zhuo, Y. & Micklefield, J. Recent advances in engineering nonribosomal peptide assembly lines. *Nature product reports* **33**, 317-347, doi:10.1039/c5np00099h (2016).
10. Weissman, K. J. Genetic engineering of modular PKSs: from combinatorial biosynthesis to synthetic biology. *Nature product reports* **33**, 203-230, doi:10.1039/c5np00109a (2016).
11. Arnison, P. G. et al. Ribosomally synthesized and post-translationally modified peptide natural products: overview and recommendations for a universal nomenclature. *Natural product reports* **30**, 108-160, doi:10.1039/c2np20085f (2013).
12. van Heel, A. J., Montalban-Lopez, M. & Kuipers, O. P. Evaluating the feasibility of lantibiotics as an alternative therapy against bacterial infections in humans. *Expert opinion on drug metabolism and toxicology* **7**, 675-680, doi :10.1517/17425255.2011.573478 (2011).
13. Ongey, E. L., Yassi, H., Pflugmacher, S. & Neubauer, P. Pharmacological and pharmacokinetic properties of lanthipeptides undergoing clinical studies. *Biotechnology letters* **39**, 473-482, doi:10.1007/s10529-016-2279-9 (2017).
14. Li, B., Sher, D., Kelly, L., Shi, Y., Huang, K., Knerr, P. J., Joewono, I., Rusch, D., Chisholm, S. W. & van der Donk, W. A. Catalytic promiscuity in the biosynthesis of cyclic peptide secondary metabolites in planktonic marine Cyanobacteria. *Proceeding of the national academy of sciences* **107**, 10430-10435, doi:10.1073/pnas.0913677107 (2010).
15. Zhang, Q., Yang, X., Wang, H. & van der Donk, W. A. High divergence of the precursor peptides in combinatorial lanthipeptide biosynthesis. *ACS chemical biology.* **9**, 2686-2694, doi:10.1021/cb500622c (2014).
16. Oman, T. J. & van der Donk, W. A. Follow the leader: the use of leader peptides to guide natural product biosynthesis. *Nature chemical biology.* **6**, 9-18, doi:10.1038/nchembio.286 (2010).
17. van Heel, A. J., Kloosterman, T. G., Montalban-Lopez, M., Deng, J., Plat, A., Baudu, B., Hendriks, D., Moll, G. N. & Kuipers, O. P. Discovery, production and modification of five novel lantibiotics using the promiscuous nisin modification machinery. *ACS synthetic biology* **5**, 1146-1154, doi:10.1021/acssynbio.6b00033 (2016).
18. Montalbán-López, M., van Heel, A. J. & Kuipers, O. P. Employing the promiscuity of lantibiotic biosynthetic machineries to produce novel antimicrobials. *FEMS microbiology review.* **41**, 5-18, doi:10.1093/femsre/fuw034 (2017).
19. Majchrzykiewicz, J. A., Lubelski, J., Moll, G. N., Kuipers, A., Bijlsma, J. J. E., Kuipers, O. P. & Rink, R. Production of a class II two-component lantibiotic of *Streptococcus pneumoniae* using the class I nisin synthetic machinery and leader sequence. *Antimicrobial agents and chemotherapy* **54**, 1498-1505, doi:10.1128/aac.00883-09 (2010).
20. Dischinger, J., Basi Chipalu, S. & Bierbaum, G. Lantibiotics: promising candidates for future applications in health care. *International journal of medical microbiology* **304**, 51-62, doi:10.1016/j.ijmm.2013.09.003 (2014).
21. Fleming, A. On the antibacterial action of cultures of a *Penicillium*, with special reference to their use in the isolation of *B. influenzae*. 1929. *Bulletin of the world health organization* **10,** 226-236 (1929).
22. Walser, M., Pellaux, R., Meyer, A., Bechtold, M., Vanderschuren, H., Reinhardt, R., Magyar, J., Pank,e S. & Held, M. Novel method for high-throughput colony PCR screening in nanoliter-reactors. *Nucleic acids research.* **37**: e57, doi:10.1093/nar/gkp160 (2009).
23. Walser, M., Leibundgut, R. M., Pellaux, R., Panke, S. & Held, M. Isolation of monoclonal microcarriers colonized by fluorescent *E. coli*. *Cytometry part A* **73A**, 788-798, doi:10.1002/cyto.a.20597 (2008).
24. Meyer, A. et al. Optimization of a whole-cell biocatalyst by employing genetically encoded product sensors inside nanolitre reactors. *Nature chemistry.* **7**, 673-678, doi:10.1038/nchem.2301 (2015).
25. Roberts, T. M., Rudolf, F., Meyer, A., Pellaux, R., Whitehead, E., Panke, S. & Held, M. Identification and characterisation of a pH-stable GFP. *Scientific reports.* **6**: 28166, doi:o.1038/srep28166 (2016).
26. Zhou, L., van Heel, A. J. & Kuipers, O. P. The length of a lantibiotic hinge region has profound influence on antimicrobial activity and host specificity. *Frontiers in microbiology* **6**: 11, doi:10.3389/fmicb.2015.00011 (2015).
27. Montalban-Lopez, M., Deng, J., van Heel, A. J. & Kuipers, O. P. Specificity and application of the lantibiotic protease NisP. *Frontiers in microbiology* **9**: 160, doi:10.3389/fmicb.2018.00160 (2018).

28. Rogers, A. Improved agar diffusion assay for nisin quantification. *Food Biotechnology* **5**, 161-168, doi:10.1111/j.1365-2672.1996.tb03242.x (1991).
29. Khosa, S., Lagedroste, M. & Smits, S. H. J. Protein defense systems against the lantibiotic nisin: function of the immunity protein NisI and the resistance protein NSR. *Frontiers in microbiology* **7**: 504, doi:10.3389/fmicb.2016.00504 (2016).
30. Khosa, S., Frieg, B., Mulnaes, D., Kleinschrodt, D., Hoeppner, A., Gohlke, H. & Smits, S.H. Structural basis of lantibiotic recognition by the nisin resistance protein from *Streptococcus agalactiae*. *Scientific reports* **6**:18679, doi:10.1038/srep18679 (2016).
31. Zhou, L., van Heel, A. J., Montalban-Lopez, M. & Kuipers, O. P. Potentiating the activity of nisin against *Escherichia coli*. *Frontiers in cell and developmental biology* **4**: 7, doi:10.3389/fcell.2016.00007 (2016).
32. Casini, A., MacDonald, J. T., De Jonghe, J., Christodoulou, G., Freemont, P.S., Baldwin, G.S. & Ellis, T. One-pot DNA construction for synthetic biology: the Modular Overlap-Directed Assembly with Linkers (MODAL) strategy. *Nucleic acids research* **42**: e7, doi:10.1093/nar/gkt915 (2014).

SI Methods

Chemicals and molecular biology

Unless otherwise noted, chemicals were obtained from Sigma-Aldrich (St. Louis, MO, USA), DNA purification kits from Zymo Research (Irvine, CA, USA) and enzymes from NEB (Ipswich, MA, USA). Sanger-sequencing was done externally (Microsynth, Balgach, Switzerland, and GATC Biotech, Konstanz, Germany) using an appropriate primer (see Supplementary Table 3 for a list of DNA oligonucleotides). For peptide and protein purifications, IMAC equilibration buffer consisted of 500 mM sodium chloride and 20 mM sodium phosphate buffer, pH 7.4; IMAC wash buffer of 20 mM imidazole, 500 mM sodium chloride and 20 mM sodium phosphate buffer, pH 7.4; IMAC elution buffer I of 500 mM sodium chloride and 475 mM sodium acetate/acetic acid buffer, pH 3.5 and IMAC elution buffer II of 500 mM imidazole, 500 mM sodium chloride and 20 mM sodium phosphate buffer, pH 7.4. Cleavage of leader peptides with NisPsol was done in NisP cleavage buffer containing 100 mM ammonium acetate/acetic acid, pH 6.0.

Bacterial strains and cultivations

Cloning was done using either *Escherichia coli* DH5α or *E. coli* DB3.1 (Thermo Fisher Scientific, Waltham, MA, USA, see Supplementary Table 4 for a list of strains) cultivated in 14 mL polypropylene tubes (Greiner, Kremsmünster, Austria), filled with 5 mL LBMiller broth (Difco, Becton Dickinson, Franklin Lakes, NJ, USA) and incubated at 37 °C with aeration on a shaker (Kuhner, Birsfelden, Switzerland) operated at 200 rpm and 25 mm amplitude. Strain *Lactococcus lactis* NZ9000, harboring the genes for NisB, NisT and NisC on plasmid pIL3BTC (see Supplementary Table 5 for a list of plasmids) was cultivated in 14 mL polypropylene tubes filled with M17 broth (Difco) supplemented with 5 g L^{-1} glucose (GM17 broth) and incubated at 30 °C without aeration. For screening and peptide production a chemically defined medium (CDM) was used. CDM contained 83.26 mM glucose, 150.00 mM 2(Nmorpholino)ethanesulfonic acid (MES), 148.87 mM sodium chloride, 0.98 mM magnesium chloride, 20.21 µM

manganese(II) chloride, 0.24 µM ammonium molybdate, 1.07 µM cobalt(II) sulfate, 1.20 µM copper(II) sulfate, 1.04 µM zinc sulfate, 20.12 µM iron(III) chloride, 9.69 µM (±)αlipoic acid, 2.10 µM Dpantothenic acid, 8.12 µM nicotinic acid, 4.91 µM pyridoxal hydrochloride, 4.86 µM pyridoxine hydrochloride, 2.96 µM thiamine hydrochloride, 0.41 µM biotin, 1.46 mM Lalanine, 1.40 mM Larginine, 0.61 mM Lasparagine, 1.03 mM Laspartic acid, 0.35 mM Lcysteine, 0.66 mM Lglutamic acid, 0.66 mM Lglutamine, 0.39 mM glycine, 0.16 mM Lhistidine, 0.63 mM Lisoleucine, 0.89 mM Lleucine, 1.02 mM Llysine, 0.26 mM Lmethionine, 0.39 mM Lphenylalanine, 3.58 mM Lproline, 1.64 mM Lserine, 0.57 mM Lthreonine, 0.18 mM Ltryptophan, 2.76 mM Ltyrosine, 0.73 mM Lvaline. Depending on the application, CDM medium was further supplemented: CDMS (for nanoFleming screening) contained in addition 9.00 mM potassium phosphate and 7.04 mM calcium chloride and was adjusted to pH 6.5 with sodium hydroxide. CDMV (for peptide precipitation) contained in addition 20.00 mM potassium phosphate, 20.00 µM calcium chloride, and 10.00 g L^{-1} tryptone and was adjusted to pH 7.0. CDMP (for peptide purification) contained in addition 20.00 mM potassium phosphate, 20.00 µM calcium chloride, 5.00 g L^{-1} tryptone and was adjusted to pH 7.0. All media were supplemented with the appropriate antibiotics for plasmid maintenance: for *E. coli*, 20 µg mL^{-1} chloramphenicol, 250 µg mL^{-1} erythromycin, and/or 50 µg mL^{-1} kanamycin; for *L. lactis*, 10 µg mL^{-1} chloramphenicol and/or 10 µg mL^{-1} erythromycin. *Micrococcus flavus* NIZO B423 was cultivated in LBMiller broth and incubated at 30 °C with aeration. The indicator strains used in inhibition zone assays, *Staphylococcus aureus* ATCC 29213 and ATCC 33591 were cultivated in cation adjusted MuellerHinton broth (MHB 2, Difco) and incubated at 37 °C with aeration. *Enterococcus faecalis* ATCC 29212 and ATCC 51575 were incubated in ToddHewitt broth (Difco) and incubated at 37 °C with aeration. *Streptococcus pneumoniae* ATCC 49619 was cultivated in ToddHewitt broth supplemented with 10% fetal bovine serum (FBS, P303302, Milian Analytica, Rheinfelden, Switzerland) and incubated at 37 °C without aeration. The strains used for MIC testing, *S. aureus* CAL and MW2, *E. faecalis* LMG 16216, *E. faecium* LMG 16003 and *Bacillus cereus* ATCC 14579 were cultivated in MuellerHinton broth (MHB, Difco). *S. pneumoniae* TIGR4 and D39 were cultivated in MHB supplemented with 5% defibrinated sheep blood (Oxoid, Thermo Fisher Scientific). The strain *L. lactis* NZ9803 displaying nisin immunity was based on *L. lactis* NZ9800 that was genome engineered to carry a deletion of the *nisP* gene using a method described previously[33]. Expression of the immunity cluster was induced by adding 5 ng mL^{-1} nisin (from a 1 mg mL^{-1} stock in 0.05% aqueous acetic acid) to the medium. Strain *L. lactis* NZ9000 [pNSR], overexpressing the nisin resistance protein from a plasmid[30] was cultivated as described for NZ9000 but adding 5 ng mL^{-1} nisin and 10 µg mL^{-1} chloramphenicol to the medium to induce the expression of the *nsr* gene and maintain the plasmid, respectively. In case cultivations were done on solid medium, 15 g L^{-1} agar (Difco) was added to the broth.

Synthesis and cloning of the DNA library

The combinatorial peptide library was synthesized without the leader peptide sequence as DNA oligonucleotide representing the antisense strand and using solid phase synthesis (see Supplementary Figure 2) by Ella Biotech GmbH (Martinsried, Germany). It was flanked by 5' and 3' primer binding site for second strand synthesis (see Supplementary Table 6 for the DNA oligonucleotide sequences of the modules). The second strand was synthesized in a primer extension reaction using the oligonucleotide mixture and the primer *lib2ndfw* in a 1:1 stoichiometric ratio (approx. 20 pmol each in 50 µl) together with 3 units of Phusion High-Fidelity DNA Polymerase (New England Biolabs, Ipswich, MA) using standard PCR reaction conditions. The double stranded product was purified using Agencourt AMPure XP beads (Beckman Coulter, Brea, CA, USA) and cloned into plasmid pSEVA241*silent*. The plasmid features transcriptional terminators 5' and 3' to the cloning site and it contains a *ccdB* expression cassette between NheI and HindIII cloning sites for efficient elimination of religands[34]. The plasmid was generated by amplifying the *ccdB* cassette using primers *ccdBBamHINheIfw* and *ccdBHindIIIrv* from plasmid pQL11 and then inserted into the multiple cloning site of pSEVA241. After plasmid proliferation in the CcdB resistant *E. coli* DB3.1 and Sanger-sequencing using primer *pSEVAt1fw* and *pSEVAtorv*, the library DNA was cloned into pSEVA241*silent* using *E. coli* DH5α. Growth of the transformants was done on large Petri dishes (145 mm diameter, Greiner) filled with 50 mL of LB-Miller agar and by plating approx. 1×10^4 colony forming units (CFUs) per plate (10 plates in total = approx. 15fold oversampling of the library). After incubation, the biomass was scraped off the plates and plasmid library pSEVA241*library* was isolated.

Next, the library was cloned into the screening plasmid pNZE3*rdmmcherry*. This plasmid was derived from plasmid pNZE3*nisA* and served as shuttle for transfer of the library from *E. coli* to *L. lactis*. The plasmid was first modified to add the gene for the red fluorescent protein mCherry. The gene was PCR-amplified from the BioBrick part BBa_J06504 in plasmid pSB1C3 using primers *mcherryNdeIfw* and *mcherry-HindIIIBamHIrv*. Next, the constitutive promoter P23[35] was PCR-amplified together with the RBS and the first 21 bases of the P23 regulated gene from the chromosome of *L. lactis* NZ9000 using primers *P23HindIII-NheIfw* and *P23NdeIrv*. Both PCR-products were digested with NdeI, ligated and the ligation-product was amplified using primers *P23HindIII-NheIfw* and *mcherryBamHIrv*, followed by a digest with NheI and BamHI. The same restriction sites were integrated into the plasmid pNZE3*nisA* using enzymatic inverse PCR[36] and the primers *pNZE3pNGNheIfw* and *pNZE3pNGBamHIrv*, which also contained a BsaI restriction site on both ends to circularize the plasmid. Next, the promoter::*mcherry* fusion was cloned into that plasmid and NheI site was removed using a modified QuickChange protocol[37] and primers *mcherry-NheIrmfw* and *mcherryNheIrmrv* to result in plasmid pNZE3*nisAmcherry*. Finally, the wild-type

nisA expression cassette was replaced by the cassette *nis-fragment-BglII-HindIII* containing the nisin-inducible promoter Pnis, the gene for the nisin leader peptide and the nisin structural gene (both genes were codon optimized for *L. lactis* MG1363) where a NheI restriction site was added between structural gene and the gene encoding for the leader peptide to facilitate the cloning of the leader-less library genes. The cassette was custom-synthesized (Geneart, Regensburg, Germany) and isolated from plasmid pMAT*nisAopt* by digesting with enzymes BglII and HindIII cloned into pNZE3*nisAmcherry* to result in plasmid pNZE3*nisAoptmcherry*. As a last step, the *nisA* structural gene was removed from that plasmid by digestion with NheI and HindIII and ligation of a random DNA-fragment, assembled by the annealing of the oligonucleotides *rdmNheIHindIIIfw* and *rdmNheIHindIIIrv* and resulted in plasmid pNZE3*rdmmcherry*. All pNZ-based plasmids were Sanger-sequenced using primers *pNZE3-seq-fw* or *pNZE3-seq-rv*.

The library was then transferred from the pSEVA241*library* to pNZE3*rdmmcherry* via NheI and HindIII to obtain the plasmid library pNZE3*librarymcherry* which was then used to transform strain *E. coli* DH5α. The transformants were grown on large Petri dishes filled with 50 mL LB-Miller agar supplemented with the appropriate antibiotics and by plating approx. 5×10^6 CFUs per plate (10 plates in total). The biomass was scraped off the plate and the plasmid was isolated. In the final step, the screening strain *L. lactis* NZ9000 [pIL3BTC] was transformed with the plasmid library to yield the candidate cells. The transformation mixture was again plated on large Petri dishes, this time filled with 50 mL GM17 agar, supplemented with the appropriate antibiotics and the cells were scraped off after growth for 48 h. The strain was diluted in liquid culture (GM17 broth, supplemented with appropriate antibiotics) to an OD_{600} of 0.5 and incubated at 30 °C for 3 h. The culture was then supplemented with glycerol to a volume fraction of 20%, 1 mL aliquots were frozen at 80 °C and the colony forming units (CFUs) of the stock were determined by plating.

Library quality control

The modular composition of the library was analyzed by next generation sequencing (Illumina MiSeq platform) at the following stages: (I) directly after second strand synthesis; (II) in plasmid pSEVA241*library* after library cloning in *E. coli*; (III) in plasmid pNZE3*librarymcherry* after library cloning in *E. coli*, and (IV) after transfer to *L. lactis*. The double-strand DNA fragment from stage I was directly used for sequencing. For stage II, III and IV, the library fragment was isolated from the plasmids by NheI and HindIII digestion followed by purification with an agarose gel. The linear DNA fragments were processed as recommended by the MiSeq Reagent Kit and sequenced in a paired-end run with 251 cycles on a MiSeq device (Illumina, San Diego, CA, USA) running RTA, version 1.18.54 (provided by the device manufacturer). Raw data were

processed using the software bcl2fastq, version 2.18.0.12 (provided by the device manufacturer) and the resulting FASTQ files from each sequencing run were processed using an in house written software to identify module counts, sequence mismatches and indels. The resulting datasets were used to judge bias and error rate of each of the synthesis and cloning steps (see Supplementary Figure 2).

nanoFleming screening

Depending on the experiment, the candidate strain either carried a plasmid for secretion of prenisin (pNZE3*nisAmcherry* = positive control), an empty plasmid (pNZE3*rdmmcherry* = negative control) or the plasmid library (pNZE3*librarymcherry*). As sensor strain, *M. flavus* (NIZO B423) or *L. lactis* NZ9000 [pNG*nisTPtdgfp*] was used. Encapsulation of cells into nLRs was done as previously described[24] using laminar-jet breakup (VAR D encapsulator from Nisco Engineering, Zürich, Switzerland) of a sodium alginate solution (20 g L^{-1} alginate in water, sterile-filtered) and using bacterial glycerol stocks. CFUs were adjusted such that on average each nLR contained 0.3 candidate cells and 150 sensor cells. The encapsulator was operated at 0.7 kHz with a flow rate of 3.3 mL min^{-1} and a nozzle diameter of 150 µm. Reactors were solidified in nLR hardening buffer (1 mM tris(hydroxymethyl)aminomethane hydrochloride (TrisHCl) pH 7.0, 100 mM $CaCl_2$) for 20 min, and briefly rinsed with nLR wash buffer (1 mM TrisHCl pH 7.0, 10 mM $CaCl_2$). The average nLR diameter after hardening was 460 µm (approx. 50 nL, CV: 4 to 7%). The nLRs where then transferred to CDMS medium (100 g nLR L^{-1} and incubated for 6 h at 30 °C on a shaker (200 rpm, 25 mm amplitude, Kuhner, Birsfelden, Switzerland). The nutrients provided in this medium are not sufficient for growth of the sensor but allow for growth of the candidate (candidate head start). After 6 h, the medium was supplemented with 5 ng mL^{-1} nisin to induce peptide production. After an additional hour of incubation, 10 g L^{-1} tryptone was added (from a 100 g L^{-1} stock in water) to allow for the growth of the sensor. Furthermore, the protease NisPsol was added (only if not already expressed by the sensor strain) at a final concentration of 0.2 µg mL^{-1} (from a 20 µg mL^{-1} enzyme stock in 100 mM MES buffer, pH 6.0). The nLRs were incubated for another hour and then removed from the medium using a cell strainer (100 µm mesh size, Falcon, Becton Dickinson, Franklin Lakes, NJ, USA) and an aliquot of approx. 1 g (wet weight, approx. 2×10^4 nLRs) was added to a 50 mL centrifugation tube pre-filled with 45 mL of a hydrophobic phase (mineral oil heavy, Carl Roth, Karlsruhe, Germany), supplemented with surfactants (40 g L^{-1} Span80 and 10 g L^{-1} Tween85). Emulsification was achieved by vigorous shaking, the whole content of the tube was poured into a large Petri dish (145 mm diameter) and incubated at 30 °C for 18 h.

After incubation, the emulsion was transferred into a sterile glass beaker and the oil was decanted. The nLRs were then transferred to 50 mL centrifugation tubes (approx.

10 mL of wet nLRs per tube) and washed several times with nLR wash buffer supplemented with 0.1 g L^{-1} Tween20, followed by centrifugation (1,000x g, 1 min) until all remaining oil was removed. The nLRs were then transferred to 50 mL of fresh nLR wash buffer and the biomass was stained (if not labeled by tdGFP) by the addition of 1 µM of SYTO 9 (from a 5 mM stock in DMSO, Thermo Fisher Scientific) followed by incubation in the dark for 1 h at room temperature at approx. 20 rpm on a benchtop roller incubator.

The nLRs were then analyzed using a large-particle flow-cytometer (BioSorter, Union Biometrica, Holliston, MA)[23]. The device was operated with water as sheath fluid and analysis was done with extinction at 488 nm as a trigger signal and recording data for time-of-flight (TOF, as a relative estimate of the particle size), extinction at 488 nm, green fluorescence (sensor, excitation laser 488 nm, beam splitter DM 562, emission filter BP 510/23 nm) and red fluorescence (candidate, excitation laser 561 nm, TR mirror, emission filter BP 615/24 nm). Signal analysis and selection of subpopulations was done using the Flow Pilot software, version 1.3.08 (provided by the device manufacturer). Data analysis was done using the FlowJo software, version 10.1 (FlowJo LLC, Ashland, OR, USA). Prior analysis of the library, samples containing nLR with embedded colonies of the positive control and negative control were analyzed. For library screening, nLRs displaying low green fluorescence intensity levels (lower than the mean green intensity of the negative control by at least 3 σ) were sorted into a 50 mL centrifugation tube prefilled with 10 mL nLR wash-buffer (device specific 'enrichment mode', max. 150 Hz sorting rate). Then, isolated nLRs were subjected to another sorting ('pure mode', max. 1 Hz sorting rate), this time spotted into Nunc MicroWell 96well plates (167008, Thermo Fisher Scientific) filled with 100 µL of GM17 broth which was supplemented with 10 µg mL^{-1} chloramphenicol and 10 µg mL^{-1} erythromycin to allow for selective recovery of the candidate strain while killing the sensor strain. The plates were sealed (airtight aluminum foil) and incubated at 30 °C for 72 h without shaking to expand the candidate strain from the nLR. Cultures in the wells were then supplemented with glycerol to a final volume fraction of 20%, the plates were sealed and frozen at 80 °C.

Fluorescence microscopy

Microscopic analysis of nLRs was carried out with the inverted fluorescence microscope Axio Observer II equipped with an AxioCam MR3 camera (Carl Zeiss Microscopy, Jena, Germany) either using bright-field or epifluorescence with filter cubes (for GFP, SYTO 9: excitation BP 470/40 nm, beam splitter DM 495 nm, emission BP 525/50 nm; for mCherry: excitation BP 565/30 nm, beam splitter DM 585 nm, emission BP 620/60 nm). Images were taken using the AxioVision software, version 4.8.2 SP3 (provided by the device manufacturer). If bright-field and epifluorescence were recorded from the same object, images were stored as overlays of both channels. Image processing and analysis was done using the Fiji software[38,39].

Peptide identification and precipitation

For each peptide, a culture in 10 mL GM17 broth inoculated from a single colony of the peptide producing strain was prepared. After growth, 6 mL of the culture was used to isolate the plasmid and the peptide gene was Sanger-sequenced using primer *pNZE3seqfw*. Next, the peptide was precipitated by trichloroacetic acid (TCA)[40]. For this, 90 mL of CDM-V medium supplemented with the appropriate antibiotics and 5 ng mL^{-1} nisin was inoculated with 900 µL from the GM17 culture. After 24 h of incubation, the cells were pelleted by centrifugation (3,200× g, 30 min). The peptide was precipitated by adding 10 mL of an ice-cold, saturated trichloroacetic acid solution (in water) to the supernatant and freezing (−20 °C) the mixture for >2 h. After thawing, the precipitated peptide was pelleted by centrifugation (48,000× g, 30 min 4 °C) and washed once with ice-cold acetone followed by a second centrifugation. The pellet was dried at room temperature and resuspended in 1 mL of an 0.05% aqueous acetic acid solution. Next, the leader peptide was cleaved off using 750 µL of the peptide solution, 250 µL of 4× NisP cleavage buffer and NisPsol at a final concentration of 0.2 µg mL^{-1} (from a 20 µg mL^{-1} enzyme stock). The mixture was incubated at 37 °C until complete cleavage was achieved (approx. 36 h, monitored by HPLCMSMS, see below). Each peptide was precipitated in duplicate.

Leader peptide quantification

The amount of leader peptide in the NisPsol treated peptide samples was quantified by HPLCMSMS using an Agilent 1200 series HPLC system coupled to an Ab Sciex 4000 QTRAP triple quadrupole mass spectrometer (operated with Analyst software, version 1.6.3, Ab Sciex, Framingham, MA) and using electrospray ionization (ESI). An aliquot of 3 µL of the peptide sample was injected onto a RPC18 column (ReproSil-Pur Basic C18 3 µm, 50 × 3 mm, Dr. Maisch, Ammerbuch, Germany), heated to 30 °C and operated with water supplemented with 0.1% formic acid as solvent A and acetonitrile supplemented with 0.1% formic acid as solvent B (all solvents MSgrade). The column was equilibrated at 10% solvent B prior injection. After injection, a gradient was imposed from 10% solvent B to 35% solvent B in 180 s at a flow rate of 800 µL min^{-1}. The column was washed with 95% solvent B for 45 s at 1,500 µL min^{-1} and equilibrated with 10% solvent B for 60 s at 1,500 µL min^{-1}. Usually three leader peptide peaks were observed: peptide 1, without methionine, resulting from cleavage by endogenous methionine aminopeptidases; peptide 2, with a non-formylated methionine at the N-terminus; peptide 3, with a formylated methionine at the N-terminus. For quantification of the leader peptides, the mass spectrometer was operated in multiple reaction monitoring (MRM) mode. The parameters for the TurboIonSpray probe: ion spray voltage (IS): 5,000 V, positive polarity, temperature (TEM): 700 °C, curtain gas (CUR): 20 psig, ion source gas 1 (GS1): 70 psig, ion source gas 2 (GS2): 60 psig, interface heater (ihe): ON and

the settings for the MS: declustering potential (DP): 80 V, entrance potential (EP): 10 V, collision energy (CE): 45 V, collision cell exit potential (CXP): 15 V and collision gas (CAD): 4 psig. Quantification was done for the fragment ion (Q3) at 574.4 m/z originating from the mother ions (Q1) from leader peptide 1 at 589.4, 784.9, 1,176.6 m/z, from leader peptide 2 at 622.0, 829.0, 1,242.5 m/z and from leader peptide 3 at 629.0, 838.0, 1,256.5 m/z with 50 ms dwell time. Signal peaks were integrated using Analyst software, version 1.6.3 (provided by the device manufacturer) and the sum of the peaks was normalized to the leader amount that resulted from a precipitated prenisin control (relative quantification). Measurements were performed in triplicate.

Inhibition zone assay

The antimicrobial activities of the precipitated peptides were confirmed using an inhibition zone assay[28]. The strains *M. flavus* (NIZO B423), *S. aureus* MSSA (ATCC 29213) and MRSA (ATCC 33591), *E. faecalis* VSE (ATCC 29212) and VRE (ATCC 51575) and *S. pneumoniae* (ATCC 49619) were used as sensor strains. Plates were assembled using 50 mL of the strain-specific agar, cooled to 40 °C and mixed with 2 mL of a culture at an OD_{600} of approx. 1. The mixture was poured into large Petri dishes (145 mm diameter) and cooled to room temperature. Using a stamp, 19 holes (3 mm diameter) were inserted into the agar and 50 µL of the samples were pipetted into each hole. Plates were incubated for 24 h and imaged using a flatbed scanner. Zone areas were measured using the Fiji software[38,39]. Inhibition zone areas were normalized to areas that resulted from a precipitated nisin control (relative quantification). Measurements were performed in triplicate.

Peptide production and purification

The leader peptide of each variant was equipped with a His_6tag followed by an additional tryptophan (HWtag, see Supplementary Table 7 for DNA and peptide sequences). The tag was integrated by enzymatic inverse PCR using primers *tagHisWBsaIfw* and *tagHisWBsaIrv*, the product was cleaved with BsaI and re-circularized by ligation. The mix was used to transform *L. lactis* NZ9000 [pIL3BTC]. The integration of the tag was confirmed by Sanger-sequencing using primer *pNZE3seqfw*.

For peptide purification, a 25 mL CDMP preculture, supplemented with the appropriate antibiotics, of the peptide producing strain was incubated overnight. Then, 20 mL of the culture was used to inoculate 2 L of CDMP medium supplemented with the same antibiotics and 10 ng mL^{-1} nisin. The culture was incubated without shaking until it reached stationary phase (after 24 to 36 h). After incubation, the cells were pelleted by centrifugation (6,000× g, 30 min). The pH of the supernatant was adjusted to 7.0, filtered through a bottle-top filter (0.22 µm pore size, PES membrane, Stericup, Merck Millipore, Billerica, MA, USA) and stored at 4 °C. The pellet was resuspended in

50 mL of 70% isopropanol, 0.4% TFA and stirred at room temperature for 2 h to separate cell-bound peptides from pellet components. After centrifugation (3,200× g, 10 min), the cell pellet was discarded and the isopropanol in the supernatant was removed with a rotary evaporator at 40 °C and 40 mbar for 10 min. The pH of the remaining solution was adjusted to 7.0 with NaOH and added to the previously retained supernatant for further treatment on an ÄKTAexplorer chromatography system (operated with Unicorn software version 5.31, GE Healthcare, Chicago, IL). The system was connected to a NiSepharose EXCEL column (XK 16/20, 10 mL bed volume, GE Healthcare) equilibrated with 5 column volumes (CV) of IMAC equilibration buffer. The culture supernatant was loaded onto the column at a flow rate of 10 mL min^1. The column was washed with 10 CV of IMAC equilibration buffer. The peptides were eluted with 3 CV of IMAC elution buffer I followed by 3 CV of IMAC elution buffer II. The whole elution fraction (60 mL) was collected and then loaded onto a Sephadex G15 column (XK 50/30, 300 mL bed volume) for desalting that was equilibrated with 5 CV of desalting buffer pH 4.0 (100 mM ammonium acetate/acetic acid buffer, pH 4). The same buffer was used for elution. The elution fraction corresponding to the peptide (monitored at 280 nm absorbance) was collected (approximately 100 mL), frozen at −80 °C for >2 h and lyophilized (approx. 60 h) using a freeze-dryer (Alpha 12 LDplus, Christ, Osterode, Germany), connected to a vacuum pump (RC6, Vacuubrand, Wertheim, Germany).

To remove the leader peptide, the freeze-dried peptides were dissolved in 40 mL of NisP cleavage buffer containing NisPsol at a concentration of 0.2 µg mL^{-1} and incubated at 37 °C for 16 h. Cleavage of the leader peptide was monitored by HPLC (see below). When incomplete, more NisPsol was added. For HPLC analysis an aliquot of 3 µL of the peptide was injected onto an RPC18 column (ReproSil-Pur 120 C18-AQ 3 µm, 150 × 2 mm, 5 × 2 mm precolumn, Dr. Maisch) heated to 30 °C and operated at a flow rate of 300 µL min^{-1} with water supplemented with 0.1% TFA as solvent A and acetonitrile supplemented with 0.1% TFA as solvent B (all solvents MSgrade). The column was equilibrated with 20% solvent B prior injection. After injection and an initial wash step of 2.8 min a gradient was imposed from 20% solvent B to 50% solvent B in 16 min. The column was washed with 95% solvent B for 5 min and equilibrated with 20% solvent B for 9.2 min. Peptide elution was monitored at an absorbance of 205, 254 and 280 nm.

HPLC-purification of the cleaved peptides was performed on an ÄKTAexplorer chromatography system. The complete peptide sample was injected onto a RPC18 column (PRONTOSIL 120 C18 10 µm, 250 × 20 mm, 50 × 20 mm precolumn, Bischoff, Leonberg, Germany), heated to 30 °C and operated at a flow rate of 10 mL min^{-1} and with water supplemented with 0.1% TFA as solvent A and acetonitrile supplemented with 0.1% TFA as solvent B. The column was equilibrated with 20% solvent B prior injection. After injection and an initial wash step of 6 min a gradient was imposed from 20% solvent B to 50% solvent B in 40 min. The column was washed with 95%

solvent B for 8 min and equilibrated with 20% solvent B for 13 min. Peptide elution was monitored at an absorbance of 205 nm and peptide peaks were collected. The fractions were frozen at −80 °C for >2 h and lyophilized (approx. 18 h) using a freeze-dryer (Alpha 2-4 LDplus, Christ), connected to a vacuum pump (RC6, Vacuubrand). In case where a peptide resulted in several peaks (e.g. due to different PTM patterns of the same translation product), all peaks were MIC-tested (see below) but only the peak with the highest activity was processed further.

NisP production

The protease was secreted as soluble form (NisPsol) where the membrane anchor of the enzyme was replaced by a His_8-tag and expressed from plasmid pNZ*nisPsol*-8H. For production, a 10 mL GM17 preculture, supplemented with the appropriate antibiotics, of the strain was used to inoculate a 1 L production culture in GM17 broth, supplemented with the same antibiotic. At an OD_{600} of 0.7, 5 ng mL^{-1} nisin was added and incubation was continued for 18 h and the culture was processed as described for the peptide purification. Purification was done on an ÄKTAexplorer chromatography system and using a Sepharose 6 Fast Flow column (GE Healthcare), loaded with Co^{2+} ions (XK 16/20, 10 mL bed volume) equilibrated with 5 CV of IMAC equilibration buffer. The supernatant was loaded onto the column at a flow rate of 5 mL min^{-1}. The column was washed with 10 CV of IMAC equilibration buffer. The protein was eluted with 6 CV of elution buffer II and fractions containing NisPsol were pooled (approx. 30 mL) and then loaded onto a Sephadex G15 column (XK 50/30, 300 mL bed volume) for desalting using a buffer containing 100 mM MES at pH 6.5. Next, glycerol was added to a final volume fraction of 10%, the protein amount was adjusted to 20 µg mL^{-1} and the protease was frozen at −80 °C.

If NisP was produced as membrane-bound variant (e.g. for *L. lactis* as sensor strain), plasmid pNG-*nisTP-gfp* was used. The plasmid is based on pNG-*nisTP* that was modified to carry the gene for tdGFP. The modification was done as described for pNZE3-*nisA-mcherry* using primers *pNZE3pNG-NheI-fw* and *pNZE3pNG-BamHI-rv* for enzymatic inverse PCR and cloning the gene for tdGFP from plasmid pKQV5-*tdgfp* using primers *tdgfp-NdeI-fw* and *tdgfp-HindIII-BamHI-rv*.

Measurement of MICs

For MIC measurements, the HPLC-purified and lyophilized peptides were resuspended in 1 mL of an 0.05% aqueous acetic acid solution and analyzed by HPLC as described above. The concentration was measured using the area under the curve at 205 nm and peptide-specific absorption properties[41,42]. For MIC assays, the bacteria were grown overnight on strain-specific agar plates. The peptides were diluted with 0.05% acetic acid to a concentration of 128 to 1024 µg mL^{-1} (depending on the strain tested). The

exact amount of peptide in the dilution was again quantified via HPLC. MICs were measured as microdilution assay in 96-well flat bottom polypropylene plates (Greiner) and performed as described by Wiegand et al.[43]. The plates were sealed (airtight aluminum foil) and incubated for 18 h without shaking at the strain-specific temperature before reading the OD_{600} using an Infinite Pro F200 plate reader (Tecan, Männedorf, Switzerland). The MIC value was set as the minimal concentration where no growth of the bacterial strain was observed (<5% of the OD_{600} value of the positive growth control in column 11). MIC experiments were performed in triplicate.

Mass-spectrometric characterization of peptides

Each peptide was analyzed twice, first to determine the number of dehydrations and second to quantify the sulfhydryl groups. The difference between the two was then used to elucidate the number of thioether-rings that must have been formed. Dehydrations were characterized by mass shifts of −18 Da, sulfhydryls were measured indirectly by derivatization of those groups with 1-cyano-4-dimethylaminopyridinium tetrafluoroborate (CDAP) resulting in a mass shift of +25 Da. For analysis, the HPLC-purified and lyophilized peptides were resuspended in 0.05% aqueous acetic acid to reach a concentration of 1 to 5 mg mL^{-1}. Next, 25 µL of the peptide was mixed with 1 µL of a 500 mM tris(2-carboxyethyl)phosphine solution (TCEP, in water, freshly prepared) in HPLC glass vials (>10-fold molar excess of TCEP) and incubated for 10 min at room temperature. For quantification of dehydrations, 24 µL of an 0.05% aqueous acetic acid solution was added and the sample was immediately measured. For quantification of sulfhydryls, 24 µL of a 178 mM CDAP (in 0.05% aqueous acetic acid, freshly prepared) was added (>100-fold molar excess of CDAP) and incubated for 30 min at room temperature prior measurement.

Measurements were performed using an Agilent 1200 series HPLC system coupled to an Ab Sciex 4000 QTRAP triple quadrupole mass spectrometer and using electrospray ionization (ESI). The device was calibrated prior measurement using the MS Chemical Kit 1, Low-High Conc. PPGs (Ab Sciex, 4406127) according to the manufacturer's recommendation. An aliquot of 2 µL of the sample was injected onto an RPC18 column (ReproSil-Pur 120 C18-AQ 3 µm, 150 × 2 mm, 5 × 2 mm precolumn, Dr. Maisch) heated to 30 °C. The HPLC parameters were the same as for the peptide quantification (see above) but using formic acid instead of TFA. The mass spectrometer was operated in Q1 mode. The parameters for the TurboIonSpray probe: ion spray voltage (IS): 5,000 V, positive polarity, temperature (TEM): 300 °C, curtain gas (CUR): 20 psig, ion source gas 1 (GS1): 70 psig, ion source gas 2 (GS2): 60 psig, interface heater (ihe): ON and the settings for the MS: declustering potential (DP): 60 V, entrance potential (EP): 10 V, collision cell rod offset (RO2): −60 V, Q3 rod offset (RO3): −62 V and exit lens (EX): −75 V.

Each sample was analyzed twice, a first explorative scan from 500 to 2,000 m z^{-1} at a scan rate of 1,000 Da s^{-1} was followed by a precise scan covering a window of 100 m z^{-1} at a scan rate of 250 Da s^{-1} for a maximum of three charge states.

The data was processed using a script written in the programming language R and employing the MALDIquant package[44]. The data was deconvoluted, averaged and centroided (signal-to-noise threshold: 5%). The results where then compared to the calculated peptide masses[41] to determine the number of dehydrations or sulfhydryl groups.

Statistical analysis

For nanoFleming screening, statistical parameters consisted of the absolute number of nLRs analyzed, the numbers of nLRs within the low and high green fluorescence subpopulations as well as the mean green fluorescence, its standard derivation (SD) and coefficient of variation (CV). All parameters were calculated using the Flow Pilot software (version 1.3.08, Union Biometrica) directly during screening. For MIC measurements, only those experiments were considered as reproducible where the spread of the three MIC values defined as $\log_2$(MICmax - MICmin) was ≤2. The statistical evaluation of the MIC values was done with a script written in the programming language R.

SI References

33. Kuipers, A., de Boef, E., Rink, R., Fekken, S., Kluskens, L. D., Driessen, A. J., Leenhouts, K., Kuipers, O. P. & Moll, G. N. NisT, the transporter of the lantibiotic nisin, can transport fully modified, dehydrated, and unmodified prenisin and fusions of the leader peptide with non-lantibiotic peptides. *Journal of biological chemistry* **279**, 22176-22182, doi:10.1074/jbc.M312789200 (2004).
34. Bernard, P. & Couturier, M. Cell killing by the F plasmid CcdB protein involves poisoning of DNA-topoisomerase II complexes. *Journal of molecular biology* **226**, 735-745, doi:10.1016/0022-2836(92)90629-x (1992).
35. van der Vossen, J. M., van der Lelie, D. & Venema, G. Isolation and characterization of Streptococcus cremoris Wg2-specific promoters. *Applied and environmental microbiology* **53**, 2452-2457 (1987).
36. Dominy, C. N. & Andrews, D. W. Site-directed mutagenesis by inverse PCR. *Methods in molecular biology* **235**, 209-223, doi:10.1385/1-59259-409-3:209 (2003).
37. Zheng, L. An efficient one-step site-directed and site-saturation mutagenesis protocol. *Nucleic acids research* **32**: e115 (2004).
38. Schindelin, J. et al. Fiji: an open-source platform for biological-image analysis. *Nature methods* **9**, 676-682, doi:10.1038/nmeth.2019 (2012).
39. Schindelin, J., Rueden, C. T., Hiner, M. C. & Eliceiri, K. W. The ImageJ ecosystem: an open platform for biomedical image analysis. *Molecular reproduction and development* **82**, 518-529, doi:10.1002/mrd.22489 (2015).
40. Green, M. R. & Sambrook, J. Molecular cloning: a laboratory manual (Fourth Edition). *Cold spring harbor laboratory press* (2012).
41. Anthis, N. J. & Clore, G. M. Sequence-specific determination of protein and peptide concentrations by absorbance at 205 nm. *Protein Science* **22**, 851-858, doi:10.1002/pro.2253 (2013).
42. Pelillo, M. et al. Calculation of the molar absorptivity of polyphenols by using liquid chromatography with diode array detection: the case of carnosic acid. *Journal of chromatography A* **1023**, 225-229, doi:10.1016/s0021-9673(03)01206-8 (2004).
43. Wiegand, I., Hilpert, K. & Hancock, R. E. Agar and broth dilution methods to determine the minimal inhibitory concentration (MIC) of antimicrobial substances. *Nature protocols* **3**, 163-175, doi:10.1038/nprot.2007.521 (2008).
44. Gibb, S. & Strimmer, K. Maldiquant: A versatile R package for the analysis of mass spectrometry data. *Bioinformatics* **28**, 2270-2271, doi:10.1093/bioinformatics/bts447 (2012).

Supplementary Figures and Tables

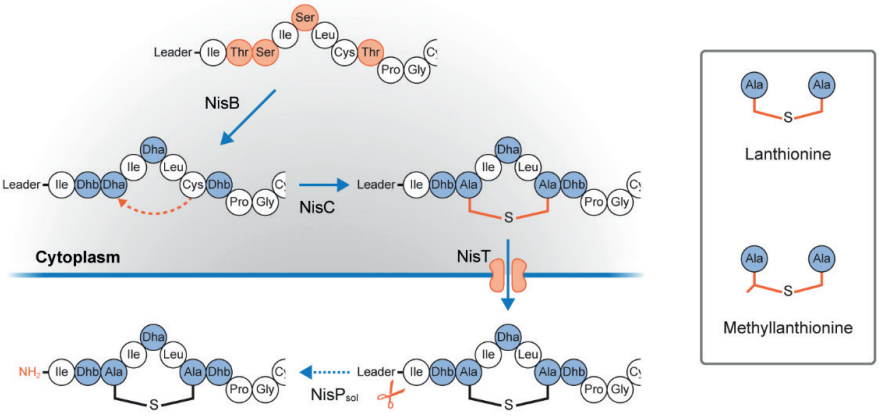

Supplementary Figure 1. Post-translational modification machinery. Four different enzymes (NisB, NisC, NisT, and NisP) were used for post-translational processing and secretion of the combinatorial peptides. Furthermore, to direct the non-modified precursor peptide synthesized at the ribosome to the modification machinery, the peptides were fused to the leader peptide of nisin. After ribosomal synthesis, the dehydratase NisB dehydrates serine and threonine residues to dehydroalanine or dehydrobutyrine, respectively. Next, the cyclase NisC catalyzes ring formation via a nucleophilic attack of a cysteine residue to the dehydroamino acids following a Michael addition type reaction mechanism leading to the formation of lanthionine (after dehydration of serine) or methyllanthionine (after dehydration of threonine). Next, NisT secretes the peptide to the extracellular space. For activation, the leader-specific protease NisP cleaves the leader peptide to release the active core peptide. Note that while wild-type NisP is membrane-bound, we used a soluble, not membrane associated variant of NisP (NisPsol) instead.

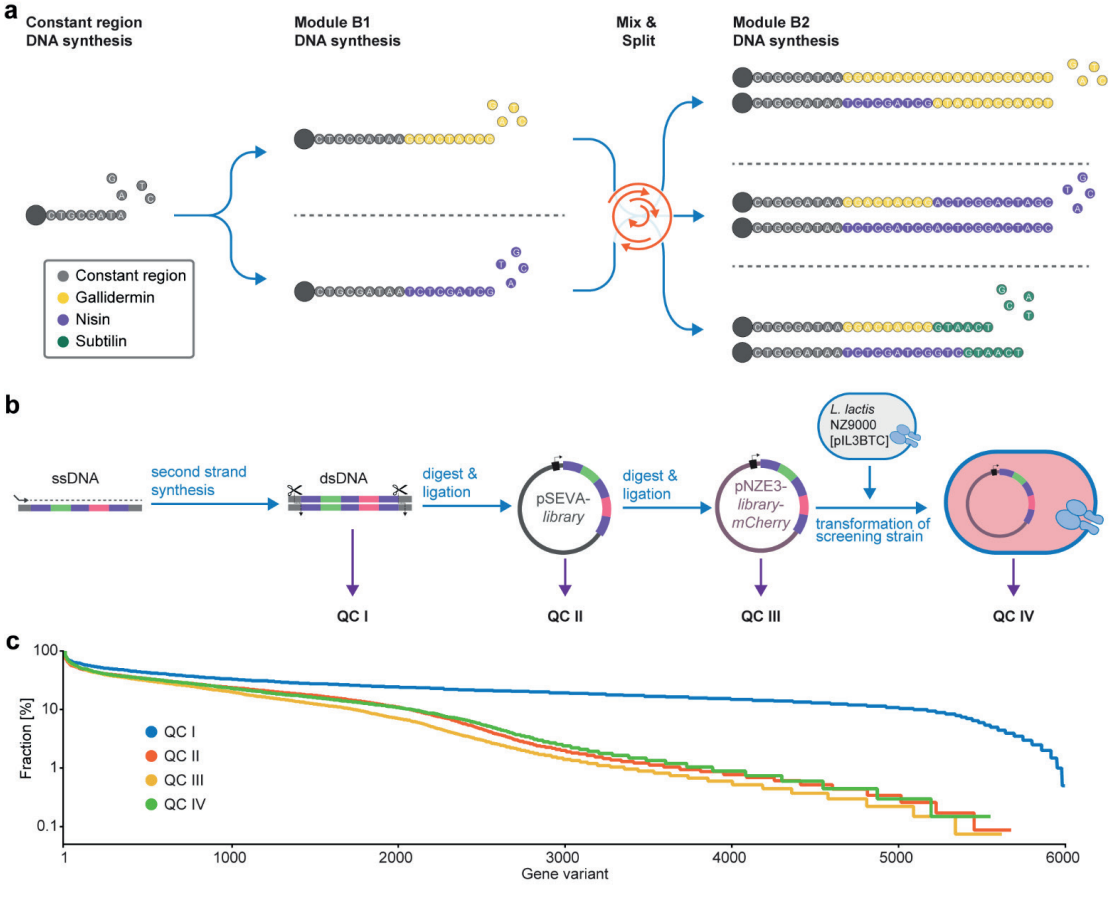
a
Constant region DNA synthesis
Module B1 DNA synthesis
Mix & Split
Module B2 DNA synthesis
Constant region
Gallidermin
Nisin
Subtilin
b
ssDNA
second strand synthesis
dsDNA
digest & ligation
pSEVA-library
digest & ligation
pNZE3-library-mCherry
L. lactis NZ9000 [pIL3BTC]
transformation of screening strain
QC I
QC II
QC III
QC IV
c
Fraction [%]
100
10
1
0.1
QC I
QC II
QC III
QC IV
1
1000
2000
3000
4000
5000
6000
Gene variant

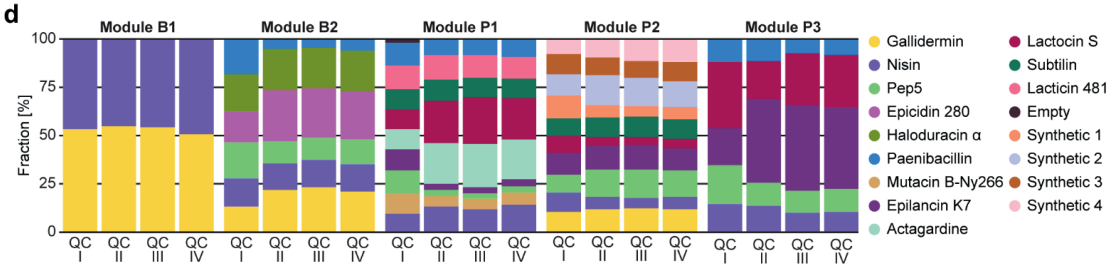

Supplementary Figure 2. Synthesis, cloning and quality control of the combinatorial library. (a) The library was generated using chemical solid phase synthesis on controlled pore glass (CPG) combined with a mix-and-split approach. We performed DNA synthesis of the antisense/minus strand of the combinatorial genes in one pot. The synthesis starts with the first module, a conserved region among the whole library (grey). This region contains restriction sites later used for cloning. After the synthesis of this constant region, the synthesis batch is, while still bound to the CPG, split up and the oligonucleotide is elongated by the synthesis of the variants of module position B1 in separate batches (yellow and violet, corresponding to the first modules of the library, gallidermin and nisin). Next the batches are pooled, mixed and separated again for the synthesis of module position B2 (yellow, violet, green). The procedure is continued until the last module is reached - which is again a constant region facilitating cloning. (b) The cloning of the combinatorial library involves several steps. First, the oligonucleotide is released from the CPG and the second strand (sense/plus strand) of the library is synthesized using an oligonucleotide complementary to the 3' constant region. After that, the double strand DNA is digested using restriction enzymes, ligated in a subcloning plasmid and proliferated in *E. coli*. The amplified plasmid is then isolated and the library fragments are excised via restriction digest, cloned into the expression plasmid and proliferated in *E. coli* again. In a last step, the plasmid is isolated from *E. coli* and transferred into the screening host *L. lactis* NZ9000 [pIL3BTC]. Every step of the protocol can result in an introduction of errors in the library (such as a shift in the modular distribution or in the accumulation of mutations). We therefore included quality control (QC) of the library composition at every processing step (indicated as QC I to IV). (c) The quality of the library is assessed via next generation sequencing with an Illumina MiSeq platform. After sequencing, every possible module combination is counted, normalized to the variant with the highest abundance and plotted. Whereas for the double stranded oligonucleotide at QC I 5,997 of 6,000 (99.95%) module combinations were found at least once for the library (NGS coverage of 44-fold), the last cloning step and after the transfer to *L. lactis* in QC IV yielded in 5,552 of 6,000 (92.5%) module combinations with counts >0 (NGS coverage of 68-fold). Moreover, the results indicate a shift in the distributions of the module combinations towards the under- and overrepresentation of certain variants. (d) Next, the distribution for each module was extracted. Whereas in QC I each module position seems to be evenly occupied by every possible module (except the 'empty' module at P1), during the first cloning step and detected at QC II, the modular composition shifts such that certain module combinations are under- and overrepresented. However, still all modules were detected and are present in the library and therefore qualifies the library for screening.

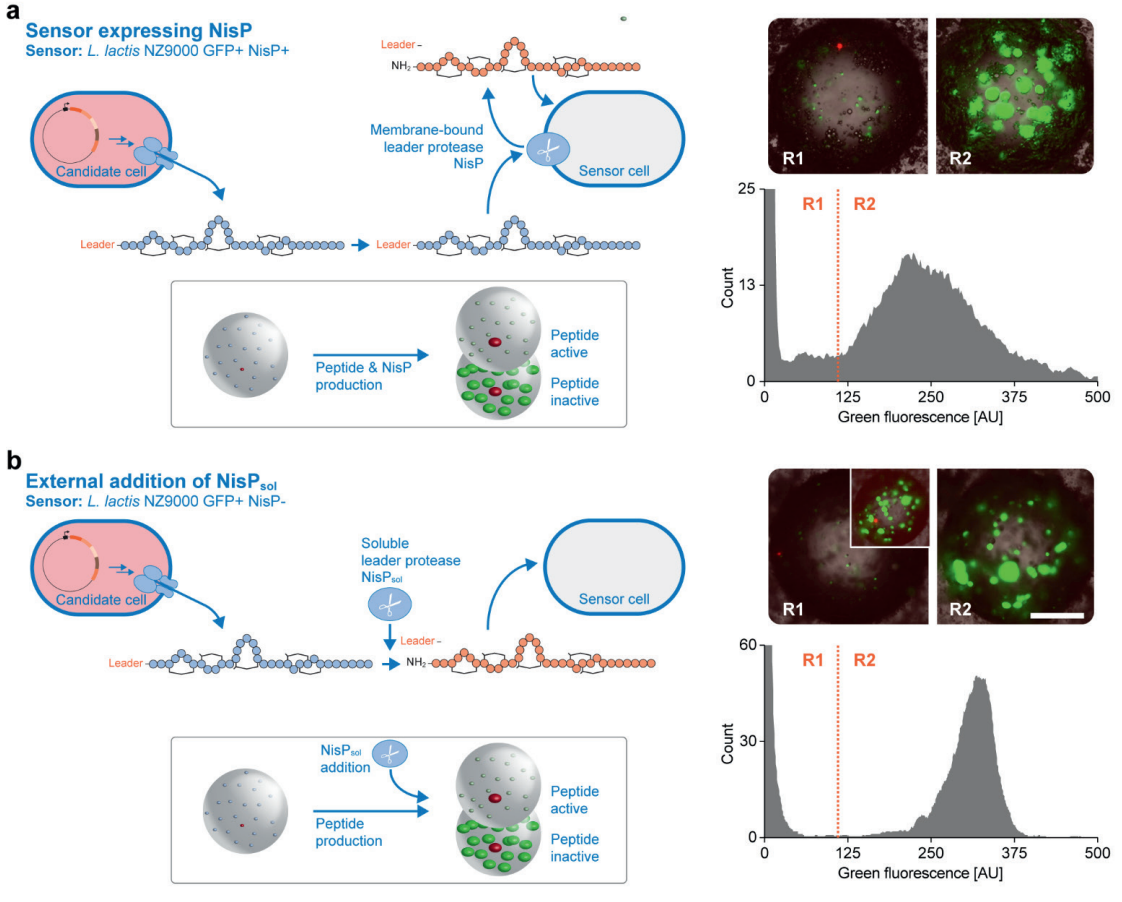
a
Sensor expressing NisP
Sensor: L. lactis NZ9000 GFP+ NisP+
Leader-
NH2
Membrane-bound
leader protease
NisP
Candidate cell
Sensor cell
Leader
Leader
Peptide & NisP
production
Peptide
active
Peptide
inactive
R1
R2
25
13
0
Count
0
125
250
375
500
Green fluorescence [AU]
b
External addition of NisPsol
Sensor: L. lactis NZ9000 GFP+ NisP-
Soluble
leader protease
NisPsol
Candidate cell
Sensor cell
Leader
Leader-
NH2
NisPsol
addition
Peptide
production
Peptide
active
Peptide
inactive
R1
R2
60
30
0
Count
0
125
250
375
500
Green fluorescence [AU]

Supplementary Figure 3. Peptide activation strategies in nLRs. The combinatorial peptides are produced and secreted bound to a leader peptide and thus still inactive. Upon secretion, the peptides diffuse within the matrix of the nLR. In order to assess their antimicrobial potency, the leader peptide has to be cleaved off. Two strategies were selected as most sui (a) The leader-specific protease NisP is heterologously produced by the sensor strain (e.g. *L. lactis* NZ9000 [pNG*nisTPtdgfp*]) and bound to the (outer) membrane of the sensor cells. Here, NisP can activate the peptides once they reach the sensor and the activated peptides can then inhibit the growth of the sensor cells. The successful implementation of this activation was shown by microscopy (images are overlays of bright-field and epifluorescence images using GFP and mCherry filter sets). The left image represents a nLR (still in the hydrophobic phase) with a prenisin producing colony (red). Reduction of green fluorescence when compared to the candidate-free nLR on the right indicates growth inhibition of the GFP-labeled sensor cells due to secretion of an active antimicrobial peptide. The same result is observed when nLRs are analyzed by large-particle flow cytometry: a separation between the two nLR-types can be achieved (R1 corresponds to nLR where an active compound is produced and R2 to candidate-free nLRs). (b) Here, a *L. lactis* strain without the gene for the leader protease NisP is used as sensor. NisP is then added as soluble enzyme from the outside of the nLR and prior incubation in the hydrophobic phase. Similar to a, the activation strategy works and leads to growth inhibition of the sensor strain in the case where a prenisin-secreting colony is present. Note that when no NisP is added to the nLR, the secreted peptide cannot be activated and no sensor growth inhibition is observed (small inset). When analyzed by large-particle flow cytometry, the separation is even more clear than in the case of heterologously expressed NisP, possibly because of the amount of protease present directly from the beginning of the incubation is higher in cases in which the protease is co-embedded rather than expressed from the sensor cells. Furthermore, the expression of *nisP* might have a negative impact on the growth of the sensor-cells and further decreases the separation of both populations. Scale bar: 200 µm.

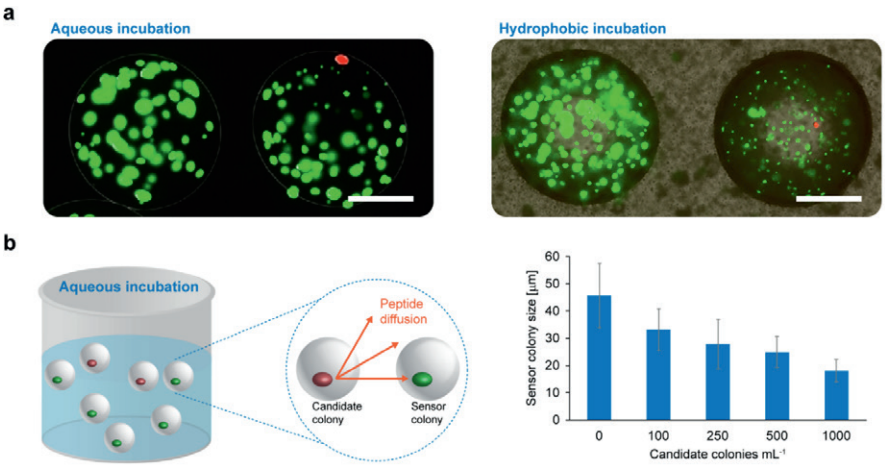

Supplementary Figure 4. Diffusion and crosstalk of nisin among nLRs. (a) Two nLR incubation methods were compared. First, the incubation of nLRs was solely done in aqueous phase (CDMS growth medium). Peptides secreted by the candidate strain *L. lactis* NZ9000 [pIL3BTC, pNZE3*nisAmcherry*] can therefore diffuse not only inside the nLR but eventually also leave the nLR which might lead to incomplete inhibition of the sensor growth inside the nLR as shown by microscopic analysis (left picture, images are overlays of bright-field and epifluorescence images using the GFP and mCherry filter set). Note the gradient of the sensor growth in the right nLR. In contrast, if incubation is performed in a hydrophobic phase (right picture), growth inhibition of the sensor is complete throughout the nLR. Scale bars: 200 µm. (b) To test whether the diffusion of peptides out of the reactors during aqueous incubation can also lead to an inhibition of cells in other nLRs in the same incubation batch we mixed nLRs containing either colonies of the candidate strain *L. lactis* NZ9000 [pIL3BTC, pNZE3-*nisA-mcherry*] or colonies of the NisP-producing sensor strain *L. lactis* NZ9000 [pNG*nisTPtdgfp*] (on average 1 colony nLR^{1}, Poisson diluted). The nLRs were then mixed in separated batches (2,000 nLR mL^{-1} each) in fixed ratios with increasing amounts of candidate-containing nLRs (0, 100, 250, 500, 1,000 nLR mL^{-1}) and decreasing numbers of sensor-containing nLRs (2,000, 1,900, 1,750, 1,500, 1,000 nLR mL^{-1}). After mixing of the nLRs in CDMS, peptide-production was induced with 5 ng mL^{-1} nisin and the nLRs where incubated for 18 h. After incubation, nLRs where recovered from the medium and the size of the sensor colonies was measured. We could observe a decreasing colony size of the sensor colonies when increasing amounts of candidate colonies were co-incubated with the sensors. This indicates a crosstalk between the nLRs allowing a diffusion of the peptides from the 'candidate' nLRs to the 'sensor' nLRs and thus inhibiting the growth of those cells. Bars represent the mean of 50 colonies (n = 50), error bars represent the standard deviation (SD).

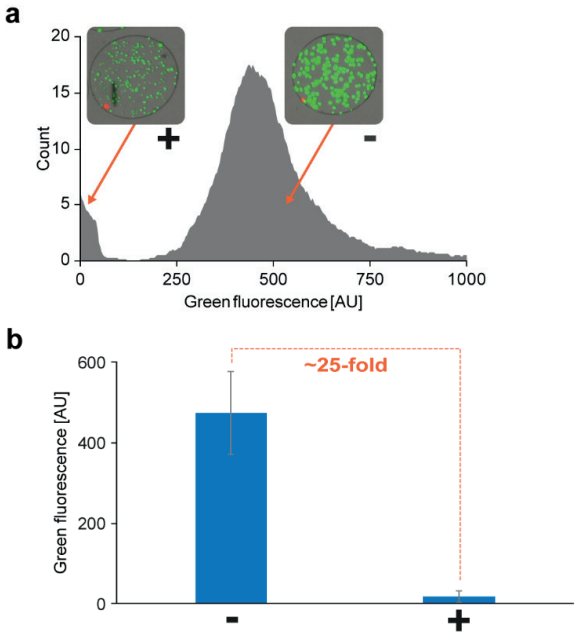

Supplementary Figure 5. Characterization of the nanoFleming assay. (a) A mixture of two different *L. lactis* strains was encapsulated. The first strain, *L. lactis* NZ9000 [pIL3BTC, pNZE3-*nisA-mcherry*] secretes prenisin (left side, '+'), and the second strain *L. lactis* NZ9000 [pIL3BTC, pNZE3-*rdm-mcherry*] does not secrete any antimicrobial peptide (right side, '-'). The cells were co-encapsulated with the NisP-producing sensor strain *L. lactis* NZ9000 [pNG-*nisTPtdgfp*], grown for 18 h in an hydrophobic phase, and then analyzed by large-particle flow cytometry, gated on the presence of a colony (as indicated by the red fluorescence of the colonies) and plotted for their green fluorescence levels. (b) Mean green fluorescent levels of the nLRs indicate a difference of approx. 25-fold between nLRs harboring a prenisin producing strain and nLRs that do not. Bars represent the mean of 71 (+) and 984 (-) nLRs (n = 71, n = 984), error bars represent the standard deviation (SD).

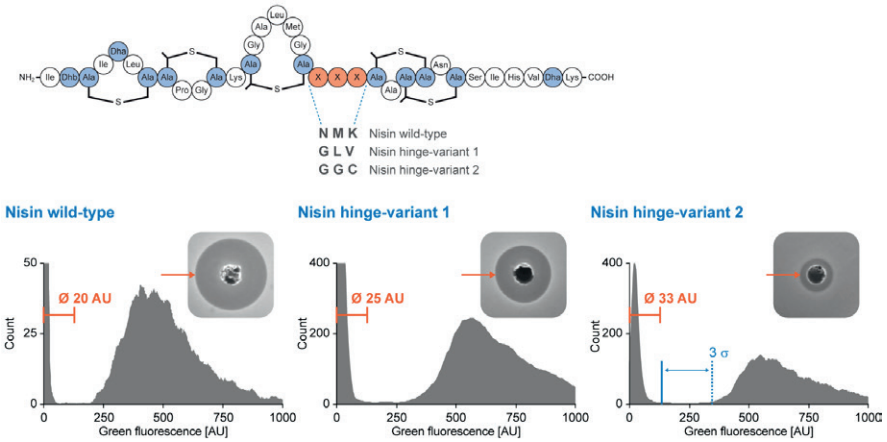

Supplementary Figure 6. Sensitivity of the nanoFleming assay. Three different nisin hinge region variants, NMK (nisin wild-type), GLV (nisin hinge-variant 1) and GGC (nisin hinge-variant 2) were produced by strain *L. lactis* NZ9000 [pIL3BTC, pNZE3-*nisA_x-mcherry*] (where x stands for the hinge region variant) and tested for their inhibition profiles against the NisP producing sensor strain *L. lactis* NZ9000 [pNG*nisTPtdgfp*] with two assay types: a standard inhibition zone assay performed on a petri dish and the nanoFleming assay. In the petri dish assay, the nisin wild-type resulted in the formation of a large halo whereas the two variants with modulated hinge regions showed a reduction in halo size. In fact, the hinge-variant 2 resulted in a halo just above the detection limit of the assay (orange arrows). When embedded in nLRs, results followed the same trend. The wild-type hinge region led to the strongest reduction in sensor growth (as measured by large-particle flow cytometry analyzing the green fluorescence of the sensor strain) here the mean green fluorescence intensity of the peak containing the nLRs with low sensor content (left fringe of the histogram) was the lowest for the wild-type hinge region (20 AU), while growth-reduction obtained from the hinge-variant 2 was considerably weaker (33 AU). However, the population not secreting a peptide (strain *L. lactis* NZ9000 [pIL3BTC, pNZE3-*rdm-mcherry*]) was well separated from the peptide secreting population in each of the three cases (>3 σ from the mean of the negative population), suggesting that the assay would also detect small amounts of antimicrobial activity.

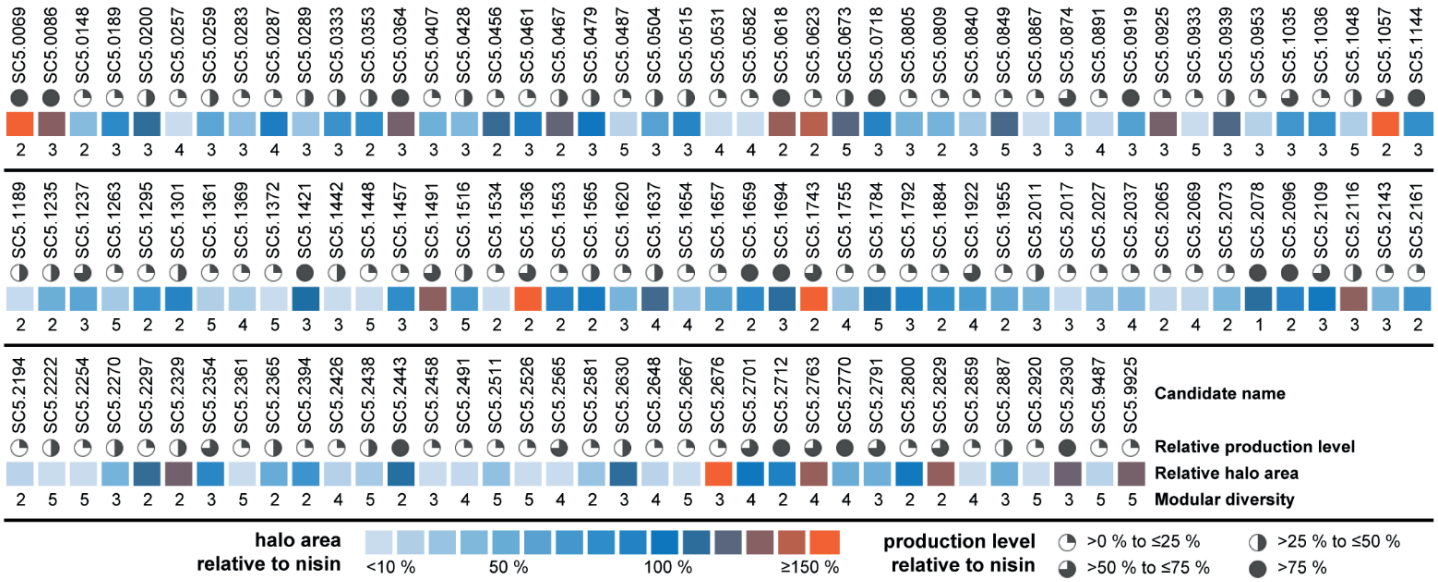

Supplementary Figure 7. Activity of peptide candidates against *M. flavus*. Summary of 126 antimicrobial peptides that were precipitated and their antimicrobial activities against *M. flavus* were determined by the size of the halo in an inhibition zone assay (100% = nisin). The production levels were approximated using HPLC-MSMS (100% = nisin).

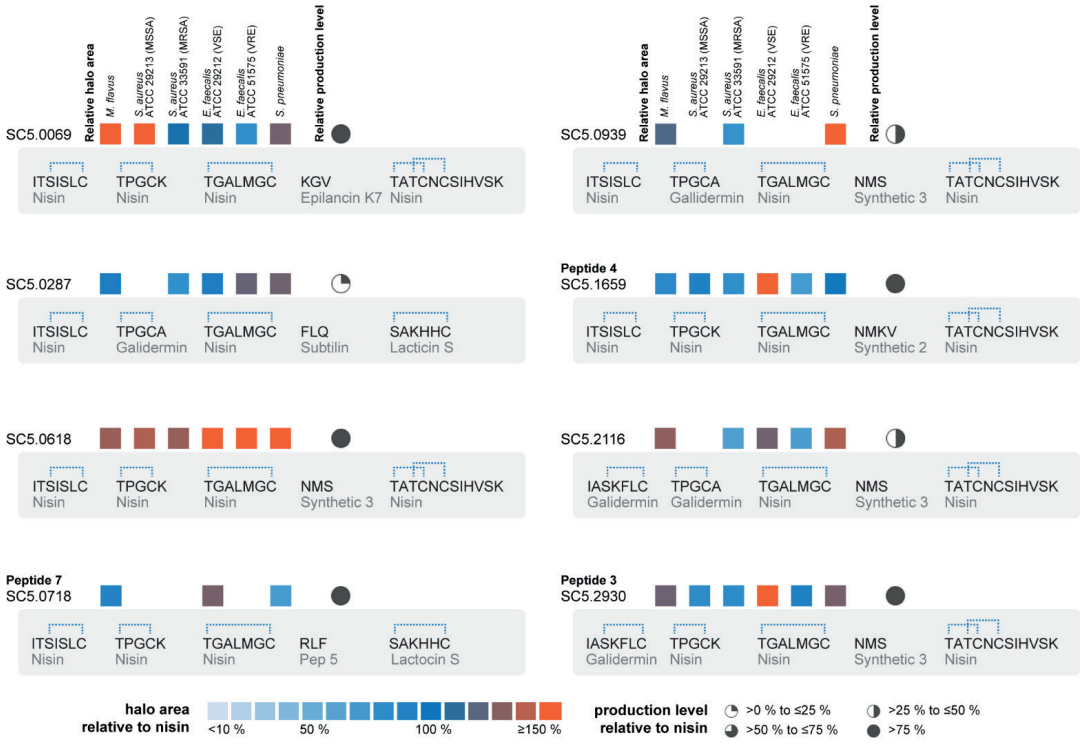

Supplementary Figure 8. Activity of peptide candidates against reference strains. Summary of 8 antimicrobial peptides that were precipitated and their antimicrobial activities against different Gram-positive reference strains were determined by the size of the halo in an inhibition zone assay (100% = nisin). The production levels were approximated using HPLC-MSMS (100% = nisin). We observed peptides with larger halos for all tested strains, e.g. SC5.0618. Other peptides show clear preference for the inhibition of a certain stain, e.g. SC5.0939 that was specifically active against *S. pneumoniae* or SC5.0287 that has nisin-like activity against most strains but not against MSSA. All peptides were precipitated in duplicate (n = 2) and antimicrobial activity and production levels were quantified in triplicate. Each dot represents the mean of those measurements.

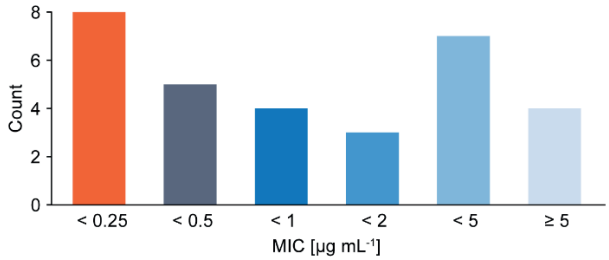

Supplementary Figure 9. MIC distribution of purified peptides against *M. flavus*. Distribution of minimal inhibitory concentrations of 31 purified peptides against *M. flavus*. Values in the histogram are means of three MIC experiments (n = 3).

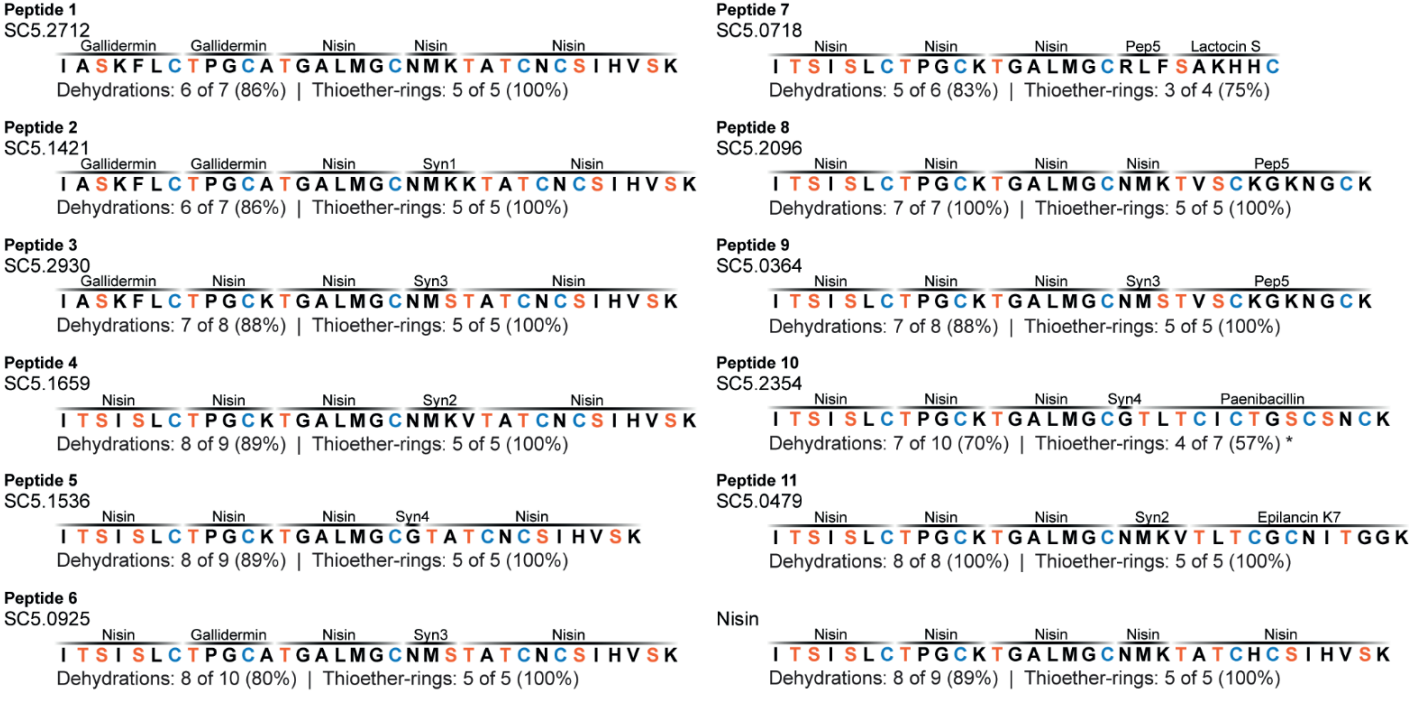

Supplementary Figure 10. Predominant modification pattern of selected peptides. Indicated are serines or threonines within the peptide that are putatively dehydrated (in orange) and can undergo thioether ring formation with cysteines (in blue). For every peptide the total number of dehydrations (each resulting in mass shift of -18 Da) was elucidated by mass spectrometry of the peptides. The number of thioether rings was detected indirectly by chemical derivatization of the peptides with 1cyano4dimethylaminopyridinium tetrafluoroborate (CDAP). CDAP only reacts with the (reduced) sulfhydryl group of cysteines, a mass shift of +25 Da therefore indicates a sulfhydryl group that is not involved in a thioether ring. In cases where variants contained a mixture of different modifications only the most predominant modification is listed. (*) Note that peptide 10 (SC5.2354) is a mixture of different dehydration and thioether patterns with a partially equal distribution (see also Supplementary Fig. 11).

a Nisin

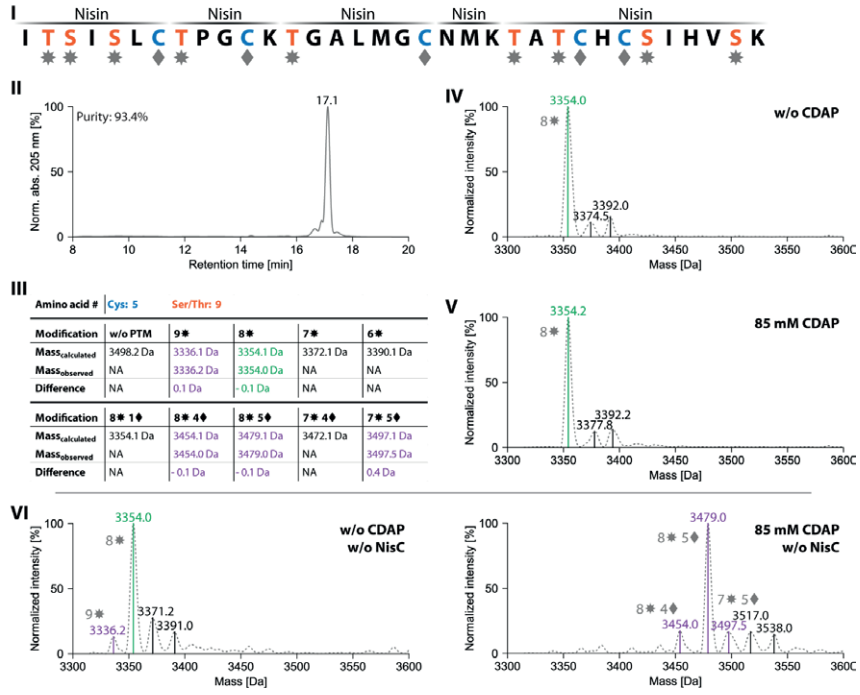

b **Peptide 1** SC5.2712

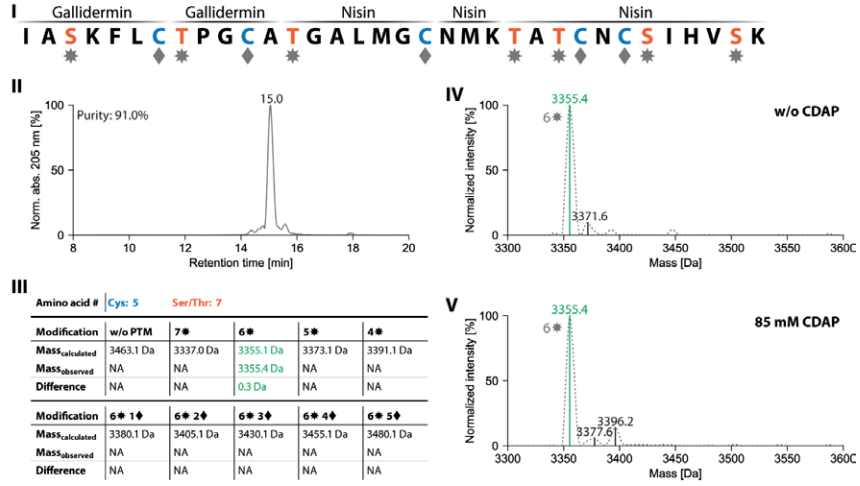

c **Peptide 2** SC5.1421

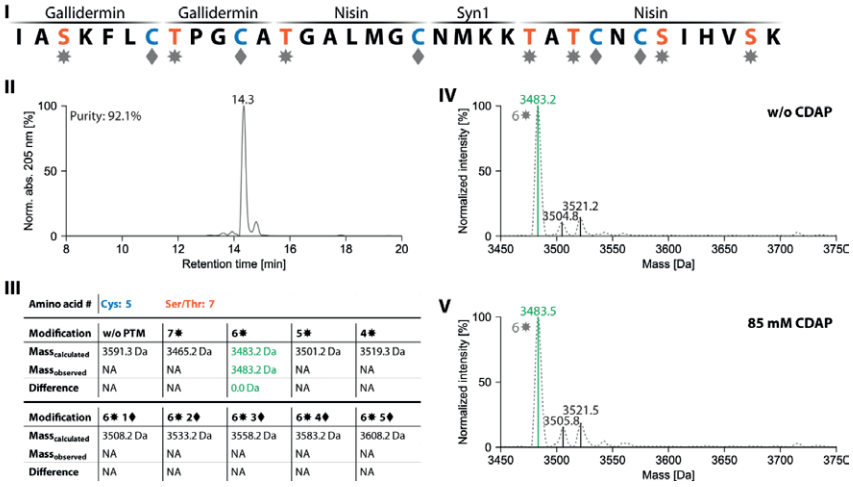

d **Peptide 3** SC5.2930

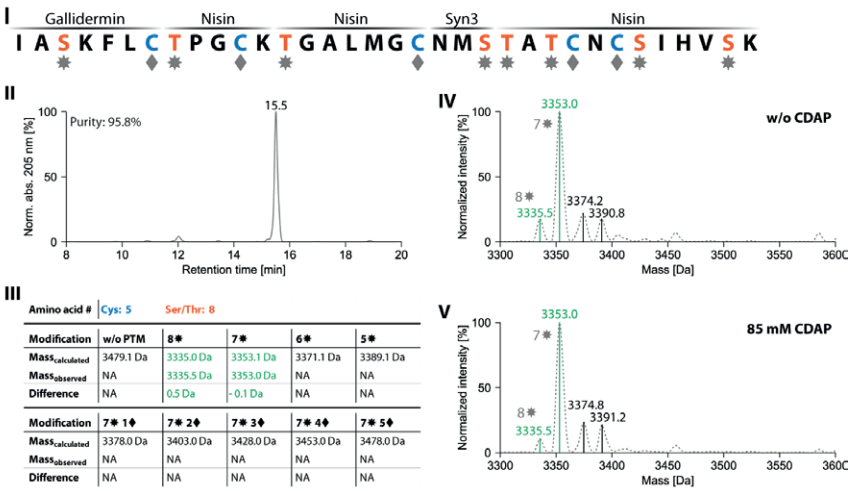

e **Peptide 4** SC5.1659

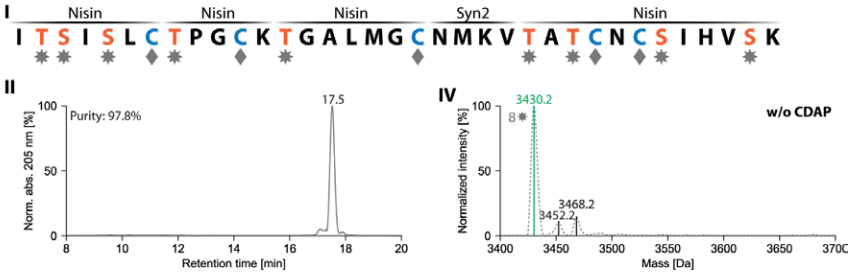

III

Amino acid #	Cys: 5	Ser/Thr: 9			
Modification	**w/o PTM**	**9✱**	**8✱**	**7✱**	**6✱**
Mass$_{calculated}$	3574.3 Da	3412.2 Da	3430.2 Da	3448.2 Da	3466.2 Da
Mass$_{observed}$	NA	NA	3430.2 Da	NA	NA
Difference	NA	NA	0.0 Da	NA	NA
Modification	**8✱ 1♦**	**8✱ 2♦**	**8✱ 3♦**	**8✱ 4♦**	**8✱ 5♦**
Mass$_{calculated}$	3455.2 Da	3480.2 Da	3505.2 Da	3530.2 Da	3555.2 Da
Mass$_{observed}$	NA	NA	NA	NA	NA
Difference	NA	NA	NA	NA	NA

f **Peptide 5** SC5.1536

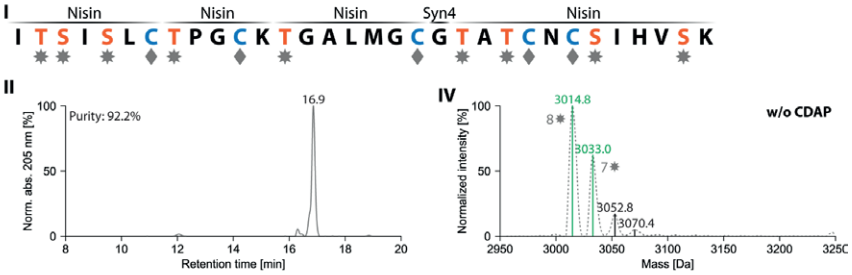

III

Amino acid #	Cys: 5	Ser/Thr: 9			
Modification	**w/o PTM**	**9✱**	**8✱**	**7✱**	**6✱**
Mass$_{calculated}$	3158.7 Da	2996.6 Da	3014.6 Da	3032.6 Da	3050.7 Da
Mass$_{observed}$	NA	NA	3014.8 Da	3033.0 Da	NA
Difference	NA	NA	0.2 Da	0.4 Da	NA
Modification	**8✱ 1♦**	**8✱ 2♦**	**8✱ 3♦**	**7✱ 1♦**	**7✱ 2♦**
Mass$_{calculated}$	3039.6 Da	3064.6 Da	3089.6 Da	3057.6 Da	3082.6 Da
Mass$_{observed}$	NA	NA	NA	3057.8 Da	NA
Difference	NA	NA	NA	0.2 Da	NA

g **Peptide 6** SC5.0925

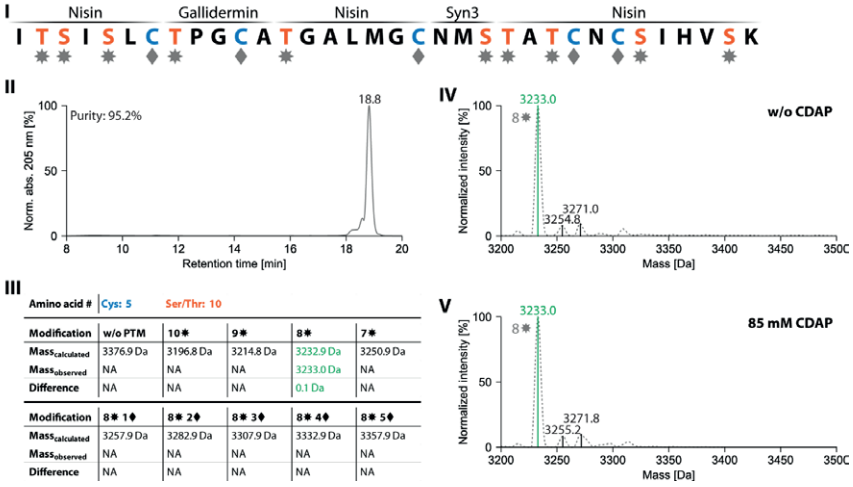

Amino acid #	Cys: 5	Ser/Thr: 10			
Modification	w/o PTM	10✱	9✱	8✱	7✱
$Mass_{calculated}$	3376.9 Da	3196.8 Da	3214.8 Da	3232.9 Da	3250.9 Da
$Mass_{observed}$	NA	NA	NA	3233.0 Da	NA
Difference	NA	NA	NA	0.1 Da	NA
Modification	8✱ 1♦	8✱ 2♦	8✱ 3♦	8✱ 4♦	8✱ 5♦
$Mass_{calculated}$	3257.9 Da	3282.9 Da	3307.9 Da	3332.9 Da	3357.9 Da
$Mass_{observed}$	NA	NA	NA	NA	NA
Difference	NA	NA	NA	NA	NA

h **Peptide 7** SC5.0718

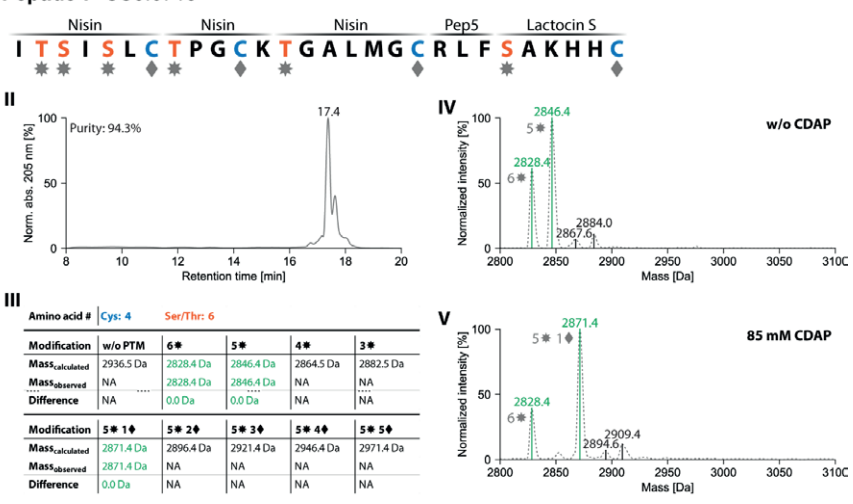

Amino acid #	Cys: 4	Ser/Thr: 6			
Modification	w/o PTM	6✱	5✱	4✱	3✱
$Mass_{calculated}$	2936.5 Da	2828.4 Da	2846.4 Da	2864.5 Da	2882.5 Da
$Mass_{observed}$	NA	2828.4 Da	2846.4 Da	NA	NA
Difference	NA	0.0 Da	0.0 Da	NA	NA
Modification	5✱ 1♦	5✱ 2♦	5✱ 3♦	5✱ 4♦	5✱ 5♦
$Mass_{calculated}$	2871.4 Da	2896.4 Da	2921.4 Da	2946.4 Da	2971.4 Da
$Mass_{observed}$	2871.4 Da	NA	NA	NA	NA
Difference	0.0 Da	NA	NA	NA	NA

I Peptide 8 SC5.2096

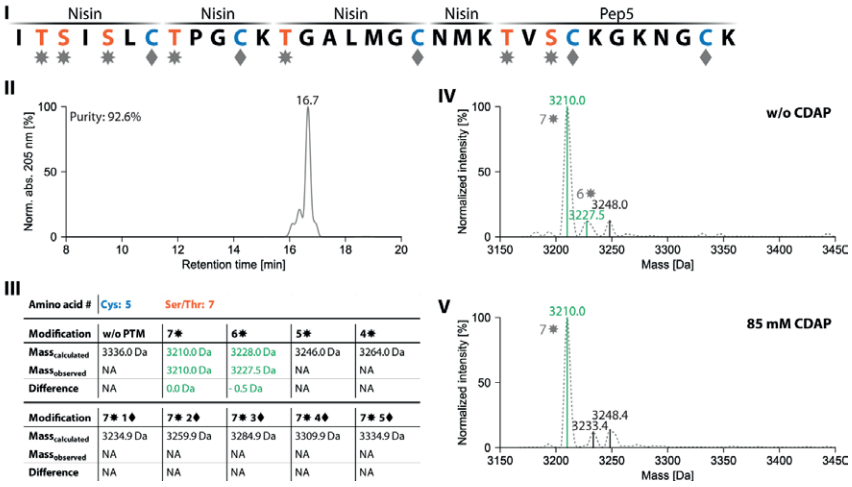

III

Amino acid #	Cys: 5	Ser/Thr: 7			
Modification	**w/o PTM**	**7✱**	**6✱**	**5✱**	**4✱**
Mass$_{calculated}$	3336.0 Da	3210.0 Da	3228.0 Da	3246.0 Da	3264.0 Da
Mass$_{observed}$	NA	3210.0 Da	3227.5 Da	NA	NA
Difference	NA	0.0 Da	- 0.5 Da	NA	NA

Modification	**7✱ 1♦**	**7✱ 2♦**	**7✱ 3♦**	**7✱ 4♦**	**7✱ 5♦**
Mass$_{calculated}$	3234.9 Da	3259.9 Da	3284.9 Da	3309.9 Da	3334.9 Da
Mass$_{observed}$	NA	NA	NA	NA	NA
Difference	NA	NA	NA	NA	NA

j Peptide 9 SC5.0364

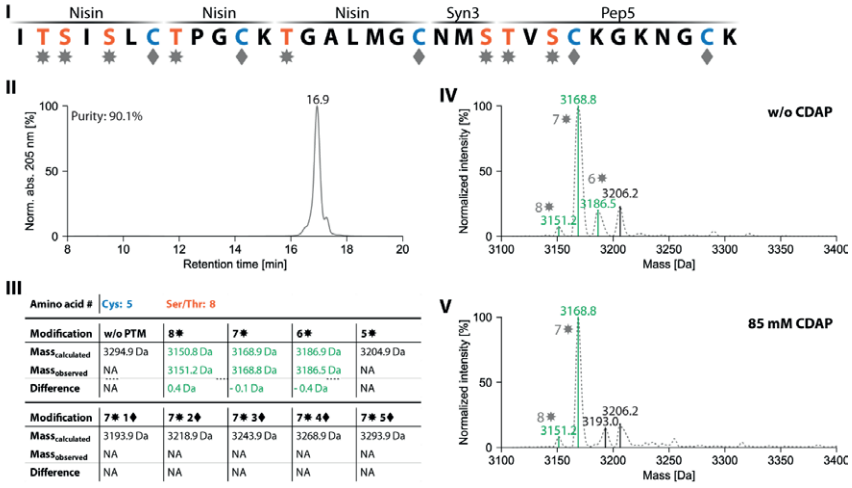

III

Amino acid #	Cys: 5	Ser/Thr: 8			
Modification	**w/o PTM**	**8✱**	**7✱**	**6✱**	**5✱**
Mass$_{calculated}$	3294.9 Da	3150.8 Da	3168.9 Da	3186.9 Da	3204.9 Da
Mass$_{observed}$	NA	3151.2 Da	3168.8 Da	3186.5 Da	NA
Difference	NA	0.4 Da	- 0.1 Da	- 0.4 Da	NA

Modification	**7✱ 1♦**	**7✱ 2♦**	**7✱ 3♦**	**7✱ 4♦**	**7✱ 5♦**
Mass$_{calculated}$	3193.9 Da	3218.9 Da	3243.9 Da	3268.9 Da	3293.9 Da
Mass$_{observed}$	NA	NA	NA	NA	NA
Difference	NA	NA	NA	NA	NA

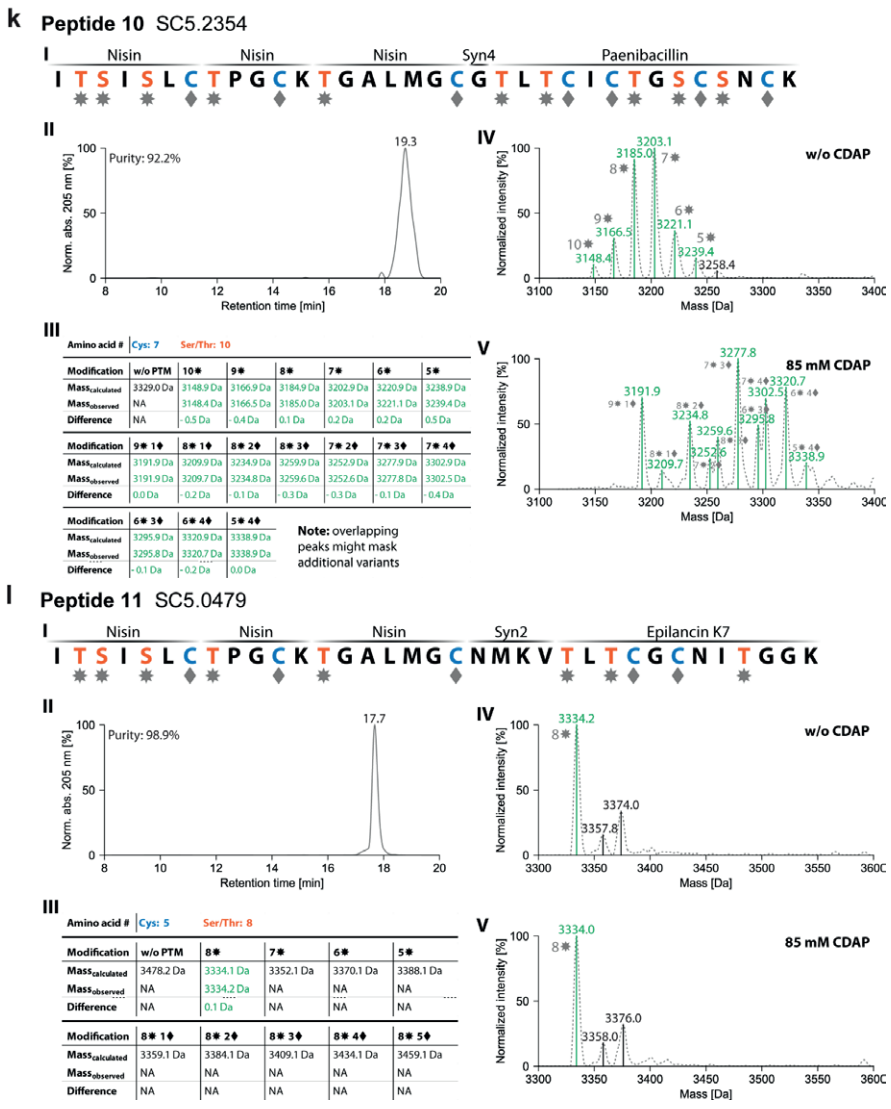

Supplementary Figure 11. Mass spectrometric characterization of selected peptides. Masses and PTMs of 12 peptides I: Amino acid sequence of the peptide; serines and threonines (in orange) can be dehydrated by NisB resulting in a mass shift of −18 Da (✱) whereas cysteine residues (in blue) that are not involved in thioether ring formation catalyzed by NisC and thus carry sulfhydryl groups can be derivatized by CDAP resulting in a mass shift of +25 Da (♦). Cysteines that do not undergo derivatization by CDAP are used to calculate the number of thioether rings that must have been formed. II: Chromatogram at 205 nm of the HPLC purified peptide. Purity at 205 nm for the main peptide peak. III: Calculated peptide masses compared to the values observed by mass spectrometry. Matches of calculated vs. observed masses (difference ≤0.5 Da) are indicated in green IV: Mass spectrum of the peptide, peaks matching the calculated peptide mass are highlighted in green. V: Mass spectrum after treatment with CDAP, peaks matching the calculated peptide mass are highlighted in green. (a) Characterization of nisin. To prove derivatization of the sulfhydryl groups by CDAP, a nisin peptide produced by a strain lacking the NisC enzyme (*L. lactis* NZ9000 [pIL3BT]) was used (VI). (b-l) Characterization of the combinatorial peptides.

Supplementary Table 1. Wild-type peptide sequences used in this study.

Peptide	Sequence
Nisin	I T S I S L C T P G C K T G A L M G C N M K T A T C H C S I H V S K
Subtilin	W K S E S L C T P GC V T G A L Q T C F L Q T L T C N C K I S K
Gallidermin	I A S K F LC T P G C A K T G S F N S Y C C
Mutacin B-Ny266	F K S W S F C T P G CA K T G S F N S Y C C
Pep5	T A G P A I R A S V K Q C Q K T L K A T R L F T V S C K G K N G C K
Epicidin 280	S L G P A I K A T R Q V C P K A T R F V T VS C K K S D C Q
Epilancin K7	S A S V L K T S I KV S K K Y C K G V T L T C G C N I T G G K
Paenibacillin	A S I I K T T I K V S K A V C K T L T C I C T G S C S N C K
Lacticin 481	K G G S G V I H T I S H E C N M N S W Q F V F T C C S
Actagardine	S S G W V C T L T I E C G T V I C A C
Lactocin S	S T P V L A S V A V S M E L L P T A S V L Y S D V A G C F K Y S A K H H C
Haloduracin α	C A W Y N I S C R L G N K G A Y C T L T V E C M P S C N

Underlined amino acids indicate the sequences used for the definition of peptide modules.

Supplementary Table 2. MICs of combinatorial peptides against *M. flavus*.

	Peptide	Module combination B1	B2	P1	P2	P3	MIC [μg mL^{-1}] *M. flavus*
	SC5.0069	Nisin	Nisin	Nisin	Epilancin K7	Nisin	0.27
	SC5.0086	Gallidermin	Gallidermin	Nisin	Synthetic 3	Nisin	0.59
	SC5.0189	Nisin	Nisin	Nisin	Synthetic 3	Epilancin K7	3.37
	SC5.0333	Nisin	Nisin	Nisin	Pep 5	Other	0.49
9	SC5.0364	Nisin	Nisin	Nisin	Synthetic 3	Pep 5	0.44
11	SC5.0479	Nisin	Nisin	Nisin	Synthetic 2	Epilancin K7	1.03
	SC5.0487	Nisin	Gallidermin	Actagardine	Epilancin K7	Pep 5	3.82
	SC5.0515	Nisin	Gallidermin	Nisin	Gallidermin	Lactocin S	3.03
	SC5.0531	Gallidermin	Gallidermin	Mutacin B-Ny266	Synthetic 4	Epilancin K7	0.55
7	SC5.0718	Nisin	Nisin	Nisin	Pep 5	Lactocin S	0.45
6	SC5.0925	Nisin	Gallidermin	Nisin	Synthetic 3	Nisin	0.87
	SC5.0953	Gallidermin	Nisin	Nisin	Synthetic 2	Nisin	0.08
	SC5.1048	Gallidermin	Nisin	Actagardine	Synthetic 3	Epilancin K7	14.1
	SC5.1237	Nisin	Nisin	Actagardine	Synthetic 3	Nisin	2.08
2	SC5.1421	Gallidermin	Gallidermin	Nisin	Synthetic 1	Nisin	0.21
	SC5.1491	Nisin	Gallidermin	Nisin	Epilancin K7	Nisin	5.11
	SC5.1516	Nisin	Gallidermin	Actagardine	EpilancinK7	Lactocin S	2.90
5	SC5.1536	Nisin	Nisin	Nisin	Synthetic 4	Nisin	0.59
	SC5.1620	Nisin	Gallidermin	Nisin	Synthetic 1	Nisin	0.33
4	SC5.1659	Nisin	Nisin	Nisin	Synthetic 2	Nisin	0.14
	SC5.1743	Nisin	Nisin	Nisin	Synthetic 3	Nisin	0.14
	SC5.1922	Gallidermin	Gallidermin	Actagardine	Synthetic 3	Epilancin K7	33.8
8	SC5.2096	Nisin	Nisin	Nisin	Nisin	Pep 5	0.18
10	SC5.2354	Nisin	Nisin	Nisin	Synthetic 4	Paenibacillin	2.95
	SC5.2630	Nisin	Nisin	Nisin	Synthetic 4	Epilancin K7	2.29
	SC5.2701	Nisin	Nisin	Paenibacillin	Synthetic 1	Lactocin S	1.49
1	SC5.2712	Gallidermin	Gallidermin	Nisin	Nisin	Nisin	0.13
	SC5.2829	Nisin	Gallidermin	Nisin	Nisin	Nisin	0.15
3	SC5.2930	Gallidermin	Nisin	Nisin	Synthetic 3	Nisin	0.04
	SC5.9487	Gallidermin	Epicidin 280	Paenibacillin	Pep 5	Nisin	1.14
	SC5.9925	Nisin	Haloduracin α	Lactocin S	Synthetic 4	Epilancin K7	73.6
	Nisin						0.07

Supplementary Table 3. DNA oligonucleotides used in this study.

ID	Name	Sequence (5' → 3')
1	*lib-2nd-fw*	GGTGCTAGCCCACGTATT
2	*ccdb-BamHI-NheI-fw*	GGATCCTCTAGAGCTAGCCCGGAATTGCCAGCTGGGGCGC
3	*ccdb-HindIII-rv*	GGCCGCAAGCTTTTATTAAATGCCCCAAAACA
4	*pSEVA-t1-fw*	TACTCAGGAGAGCGTTCACC
5	*pSEVA-to-rv*	GGGGACCCCTGGATTCTCAC
6	*mcherry-NdeI-fw*	TGCAGCTcatatgCATAGCAAGGGC
7	*mcherry-HindIII-BamHI-rv*	TGAGCAaagcttggatccTTATTACTTGTACAGCTC
8	*P23-HindIII-NheI-fw*	TAATATaagcttgctagcTCGAAAAGCCCTG
9	*P23-NdeI-rv*	AGCGCAcatatgATCATTGTCATTCATATTTT
10	*pNZE3pNG-NheI-fw*	TAATGGTCTCTgtatacGCTAGCttctcgagtgcatattttc
11	*pNZE3pNG-BamHI-rv*	TAATGGTCTCTgtatacGGATCCgttatcggtcctttaattg
12	*mcherry-NheI-rm-fw*	GTCAGGGCTTTTCGAGGCAGCttctcgagtgc
13	*mcherry-NheI-rm-rv*	gcactcgagaaGCTGCCTCGAAAAGCCCTGAC
14	*nis-fragment-BglII-HindIII*	agatctagtcttataactatactgacaatagaaacattaacaaatctaaaacagtcttaattctatct tgagaaagtattggtaataatattattgtcgataacgcgagcataataaacggctctgattaaattc tgaagtttgttagatacaatgatttcgttcgaaggaactacaaaataaattataaggaggcactca ccatgtcaacaaaagattttaatcttgatcttgtttcagtttcaaaaaaagattcaggtgctagccca cgtattacttcaatttcactttgtactccaggttgtaaaactggtgctcttatgggttgtaatatgaa aactgctacttgtcattgttcaattcatgtttcaaaatgataagctt
15	*rdm-NheI-HindIII-fw*	[P]ctagcTAATCATCTAACATGGGATTTGCTATAACTCTTGAA CGCTACATGTACGAAACCATATTAa
16	*rdm-NheI-HindIII-rv*	[P]agcttTAATATGGTTTCGTACATGTAGCGTTCAAGAGTTAT AGCAAATCCCATGTTAGATGATTAg
17	*pNZE3-seq-fw*	aaacatgcaggaattgacga
18	*pNZE3-seq-rv*	ggcttttacgctacgataac
19	*tag-HisW-BsaI-fw*	atcttcGGTCTCtCATCACCATCACTGGtcaacaaaagattttaatcttg
20	*tag-HisW-BsaI-rv*	tccaatGGTCTCtGATGGTGATGcatggtgagtgcctcc
21	*tdgfp-NdeI-fw*	TGCAGCTcatatgAGTAAACGAGAAGAACT
22	*tdgfp-HindIII-BamHI-rv*	TGAGCAaagcttggatccTTATTTGTAGAGCTCAT

Underlined bases indicate restriction sites (see oligonucleotide name for enzyme).
[P] indicates a phosphorylation of the hydroxyl group at the terminal base of the oligonucleotide.

Supplementary Table 4. Bacterial strains used in this study.

ID	Name	Genotype	Reference
1	*M. flavus* NIZO B423		NIZO food research
2	*L. lactis* NZ9000	MG1655 *pepN*::*nisRnisK*	1
3	*L. lactis* NZ9800	NZ9700 Δ*nisA*	2
4	*L. lactis* NZ9803	NZ9800 Δ*nisP* Δ*nisA*	This work
5	*S. aureus* ATCC 29213	methicillin sensitive (MSSA)	3
6	*S. aureus* ATCC 33591	methicillin resistant (MRSA)	3,4
7	*S. aureus* CAL	methicillin resistant (MRSA)	The University Medical Center Groningen, The Netherlands
8	*S. aureus* MW2	methicillin resistant (MRSA)	The University Medical Center Groningen, The Netherlands
9	*E. faecalis* ATCC 29212	vancomycin sensitive (VSE)	3
10	*E. faecalis* ATCC 51575	gentamicin, streptomycin, and vancomycin resistant (VRE)	3,5
11	*E. faecalis* LMG 16216	vancomycin resistant (VRE)	Laboratory of Microbiology, Gent, Belgium
12	*E. faecium* LMG 16003	avoparcin and vancomycin resistant (VRE)	Laboratory of Microbiology, Gent, Belgium
13	*S. pneumoniae* ATCC 49619	serotype 19F	3
14	*S. pneumoniae* D39	serotype 2	6
15	*S. pneumoniae* TIGR4	serotype 4	7
16	*B. cereus* ATCC 14579		8
17	*E. coli* DH5α	F^- Φ80 *lacZ*ΔM15 Δ(*lacZYA-argF*)*U169 recA1 endA1 hsdR17*(rK^-, mK^+) *phoA supE44* λ^- *thi-1 gyrA96 relA1*	9
18	*E. coli* DB3.1	F^- *gyrA462 endA1 glnV44* Δ(*sr1-recA*) *mcrB mrr hsdS20*(rB^-, mB^-) *ara14 galK2 lacY1 proA2 rpsL20*(Sm^r) *xyl5* Δ*leu mtl1*	10,11

Supplementary Table 5. Plasmids used in this study.

ID	Name	Features	Reference
1	pIL3BTC	pAMβ1 origin of replication, chloramphenicol resistance, expression of *nisBTC* under control of the P*nis* promoter	12
2	pNSR	pNZ-SV-*Sa*NSR, pSH71 origin of replication, chloramphenicol resistance, *L. lactis – E. coli* shuttle, expression of *nsr* under control of the P*nis* promoter	13,14
3	pEmpty	pNZ8048, pSH71 origin of replication, chloramphenicol resistance, *L. lactis – E. coli* shuttle, P*nis* promoter and empty multiple cloning site	1
4	pQL11	pUC origin of replication, ampicillin resistance, carries the *ccdB* expression cassette	15
5	pSEVA241	ColE1 origin of replication, kanamycin resistance	16
6	pSEVA241-*silent*	as pSEVA241, carries cassette for *ccdB* expression	This work
7	pSEVA241-*library*	as pSEVA241, carries the leader-less library	This work
8	pNZE3-*nisA*	pSH71 origin of replication, erythromycin resistance, *L. lactis – E. coli* shuttle, expression of *nisA* under control of the P*nis* promoter	17
9	pSB1C3-BBa_J06504	pMB1 origin of replication, chloramphenicol resistance, carries the gene for mCherry (BioBrick part BBa_J06504)	18,19
10	pNZE3-*nisA-mcherry*	as pNZE3-*nisA*, expression of *mcherry* under control of the P23 promoter	This work
11	pMA-T-*nisAopt*	pRO1600/ColE1 origin of replication, ampicillin resistance, carries a codon-optimized nisin leader and *nisA* gene	This work
12	pNZE3-*nisA-opt-mcherry*	as pNZE3-*nisA-mcherry*, carries a codon-optimized nisin leader and *nisA* gene separated by a NheI site for cloning and fused to the P*nis* promoter	This work
13	pNZE3-*rdm-mcherry*	as pNZE3-*nisAopt-mcherry*, carries a random sequence instead of the *nisA* structural gene	This work
14	pNZE3-*library-mcherry*	as pNZE3-*nisAopt-mcherry*, carries the library instead of the *nisA* structural gene	This work
15	pIL3BT	pIL3BTC derived, lacking the gene for NisC	20
16	pNZ-*nisPsol*-8H	pSH71 origin of replication, chloramphenicol resistance, *L. lactis – E. coli* shuttle, expression of *nisP* with His_8-tag under control of the P*nis* promoter	21
17	pNG-*nisTP*	pSH71 origin of replication, chloramphenicol resistance, *L. lactis – E. coli* shuttle, expression of *nisP* under control of the P*nis* promoter	17
18	pKQV5-*tdgfp*	pBR322 origin of replication, ampicillin resistance, expression of *tdgfp* under control of the Ptac promoter	22
19	pNG-*nisTP-tdgfp*	as pNG-*nisTP*, expression of *tdgfp* under control of the P23 promoter	This work

Supplementary Table 6. DNA sequences of peptide modules.

Origin	5'-const.	Module B1	Module B2	Module P1	Module P2	Module P3	3'-const.
Constant regions	GGTGCTAGC CCACGT						TGATAAGCTT TCTTTGAAC
Nisin		ATTACTTCGAT CTCATTGTGT	ACACCTGGTT GTAAA	ACAGGTGCACT TATGGGTTGT	AATATGAAA	ACAGCTACTTGTAATTGT TCAATTCACGTTTCAAAA	
Subtilin				TGGAAATCAGA ATCTCTTTGC	TTCCTTCAA		
Gallidermin		ATTGCATCAAA ATTTCTTTGT	ACTCCAGGTT GTGCA		AAAACAGGT		
Mutacin B-Ny266				TTTAAATCTTGG AGCTTTTGT			
Pep5			TCAGTAAAAC AATGTCAA	AAAACATTAAAA GCTACA	CGCCTTTTT	ACAGTTTCATGTAAAGGT AAAAACGGATGTAAA	
Epicidin 280			ACACGTCAAG TTTGTCCA				
Epilancin K7				TCAAAAAAATAT TGC	AAAGGTGTT	ACATTGACATGTGGATGC AACATCACAGGAGGTAAA	
Paenibacillin			ACTACAATTA AAGTT	TCAAAAGCAGTT TGT		ACATTGACATGTATTTGTACA GGTTCATGTTCAAATTGTAAG	
Lacticin 481				AAAGGTGGTTCT GGAGTTATTCAT			
Actagardine				TCATCAGGTTGG GTTTGC			
Lactocin S				TCTGATGTGGCTG GCTGT	TTCAAATAT	TCAGCTAAACATCACTGC	
Halodura-cin α			ACTTTGACAG TTGAGTGT				
Empty				n/a			
Synthetic 1					AATATGAAAAAA		
Synthetic 2					AACATGAAAGTC		
Synthetic 3					AATATGTCA		
Synthetic 4					GGT		

Underlined bases indicate restriction sites; "n/a" indicates an empty module position that is left out during synthesis.

Supplementary Table 7. Amino acid and DNA sequences of combinatorial peptides.

ID	Sequence
SC5.0069	**AA:** ITSISLCTPGCKTGALMGCKGVTATCNCSIHVSK
	DNA: ATTACTTCGATCTCATTGTGTACACCTGGTTGTAAAACAGGTGCACTTATG GGTTGTAAAGGTGTTACAGCTACTTGTAATTGTTCAATTCACGTTTCAAAA
SC5.0086	**AA:** IASKFLCTPGCATGALMGCNMSTATCNCSIHVSK
	DNA: ATTGCATCAAAATTTCTTTGTACTCCAGGTTGTGCAACAGGTGCACTTATG GGTTGTAATATGTCAACAGCTACTTGTAATTGTTCAATTCACGTTTCAAAA
SC5.0189	**AA:** ITSISLCTPGCKTGALMGCNMSTLTCGCNITGGK
	DNA: ATTACTTCGATCTCATTGTGTACACCTGGTTGTAAAACAGGTGCACTTATG GGTTGTAATATGTCAACATTGACATGTGGATGCAACATCACAGGAGGTAAA
SC5.0333	**AA:** ITSISLCTPGCKTGALMGCRLFTVSCKGKKRM
	DNA: ATTACTTCGATCTCATTGTGTACACCTGGTTGTAAAACAGGTGCACTTATG GGTTGTCGCCTTTTTACAGTTTCATGTAAAGGTAAAAAACGGATG
Peptide 9 SC5.0364	**AA:** ITSISLCTPGCKTGALMGCNMSTVSCKGKNGCK
	DNA: ATTACTTCGATCTCATTGTGTACACCTGGTTGTAAAACAGGTGCACTTATG GGTTGTAATATGTCAACAGTTTCATGTAAAGGTAAAAACGGATGTAAA
Peptide 11 SC5.0479	**AA:** ITSISLCTPGCKTGALMGCNMKVTLTCGCNITGGK
	DNA: ATTACTTCGATCTCATTGTGTACACCTGGTTGTAAAACAGGTGCACTTATG GGTTGTAACATGAAAGTCACATTGACATGTGGATGCAACATCACAGGAGGTAAA
SC5.0487	**AA:** ITSISLCTPGCASSGWVCKGVTVSCKGKNGCK
	DNA: ATTACTTCGATCTCATTGTGTACTCCAGGTTGTGCATCATCAGGTTGGGTT TGCAAAGGTGTTACAGTTTCATGTAAAGGTAAAAACGGATGTAAA
SC5.0515	**AA:** ITSISLCTPGCATGALMGCKTGSAKHHC
	DNA: ATTACTTCGATCTCATTGTGTACTCCAGGTTGTGCAACAGGTGCACTTATG GGTTGTAAAACAGGTTCAGCTAAACATCACTGC
SC5.0531	**AA:** IASKFLCTPGCAFKSWSFCGTLTCGCNITGGK
	DNA: ATTGCATCAAAATTTCTTTGTACTCCAGGTTGTGCATTTAAATCTTGGAGC TTTTGTGGTACATTGACATGTGGATGCAACATCACAGGAGGTAAA
Peptide 7 SC5.0718	**AA:** ITSISLCTPGCKTGALMGCRLFSAKHHC
	DNA: ATTACTTCGATCTCATTGTGTACACCTGGTTGTAAAACAGGTGCACTTATG GGTTGTCGCCTTTTTTCAGCTAAACATCACTGC
Peptide 6 SC5.0925	**AA:** ITSISLCTPGCATGALMGCNMSTATCNCSIHVSK
	DNA: ATTACTTCGATCTCATTGTGTACTCCAGGTTGTGCAACAGGTGCACTTATG GGTTGTAATATGTCAACAGCTACTTGTAATTGTTCAATTCACGTTTCAAAA
SC5.0953	**AA:** IASKFLCTPGCKTGALMGCNMKVTATCNCSIHVSK
	DNA: ATTGCATCAAAATTTCTTTGTACACCTGGTTGTAAAACAGGTGCACTTATG GGTTGTAACATGAAAGTCACAGCTACTTGTAATTGTTCAATTCACGTTTCAAAA
SC5.1048	**AA:** IASKFLCTPGCKSSGWVCNMSTLTCGCNITGGK
	DNA: ATTGCATCAAAATTTCTTTGTACACCTGGTTGTAAATCATCAGGTTGGGTT TGCAATATGTCAACATTGACATGTGGATGCAACATCACAGGAGGTAAA
SC5.1237	**AA:** ITSISLCTPGCKSSGWVCNMSTATCNCSIHVSK
	DNA: ATTACTTCGATCTCATTGTGTACACCTGGTTGTAAATCATCAGGTTGGGTT TGCAATATGTCAACAGCTACTTGTAATTGTTCAATTCACGTTTCAAAA
Peptide 2 SC5.1421	**AA:** IASKFLCTPGCATGALMGCNMKKTATCNCSIHVSK
	DNA: ATTGCATCAAAATTTCTTTGTACTCCAGGTTGTGCAACAGGTGCACTTATG GGTTGTAATATGAAAAAAACAGCTACTTGTAATTGTTCAATTCACGTTTCAAAA

ID	Sequence
SC5.1491	**AA:** ITSISLCTPGCATGALMGCKGVTATCNCSIHVSK
	DNA: ATTACTTCGATCTCATTGTGTACTCCAGGTTGTGCAACAGGTGCACTTATG GGTTGTAAAGGTGTTACAGCTACTTGTAATTGTTCAATTCACGTTTCAAAA
SC5.1516	**AA:** ITSISLCTPGCASSGWVCKGVSAKHHC
	DNA: ATTACTTCGATCTCATTGTGTACTCCAGGTTGTGCATCATCAGGTTGGGTT TGCAAAGGTGTTTCAGCTAAACATCACTGC
Peptide 5 SC5.1536	**AA:** ITSISLCTPGCKTGALMGCGTATCNCSIHVSK
	DNA: ATTACTTCGATCTCATTGTGTACACCTGGTTGTAAAACAGGTGCACTTATG GGTTGTGGTACAGCTACTTGTAATTGTTCAATTCACGTTTCAAAA
SC5.1620	**AA:** ITSISLCTPGCATGALMGCNMKKTATCNCSIHVSK
	DNA: ATTACTTCGATCTCATTGTGTACTCCAGGTTGTGCAACAGGTGCACTTATG GGTTGTAATATGAAAAAAACAGCTACTTGTAATTGTTCAATTCACGTTTCAAAA
Peptide 4 SC5.1659	**AA:** ITSISLCTPGCKTGALMGCNMKVTATCNCSIHVSK
	DNA: ATTACTTCGATCTCATTGTGTACACCTGGTTGTAAAACAGGTGCACTTATG GGTTGTAACATGAAAGTCACAGCTACTTGTAATTGTTCAATTCACGTTTCAAAA
SC5.1743	**AA:** ITSISLCTPGCKTGALMGCNMSTATCNCSIHVSK
	DNA: ATTACTTCGATCTCATTGTGTACACCTGGTTGTAAAACAGGTGCACTTATG GGTTGTAATATGTCAACAGCTACTTGTAATTGTTCAATTCACGTTTCAAAA
SC5.1922	**AA:** IASKFLCTPGCASSGWVCNMSTLTCGCNITGGK
	DNA: ATTGCATCAAAATTTCTTTGTACTCCAGGTTGTGCATCATCAGGTTGGGTT TGCAATATGTCAACATTGACATGTGGATGCAACATCACAGGAGGTAAA
Peptide 8 SC5.2096	**AA:** ITSISLCTPGCKTGALMGCNMKTVSCKGKNGCK
	DNA: ATTACTTCGATCTCATTGTGTACACCTGGTTGTAAAACAGGTGCACTTATG GGTTGTAATATGAAAACAGTTTCATGTAAAGGTAAAAACGGATGTAAA
Peptide 10 SC5.2354	**AA:** ITSISLCTPGCKTGALMGCGTLTCICTGSCSNCK
	DNA: ATTACTTCGATCTCATTGTGTACACCTGGTTGTAAAACAGGTGCACTTATG GGTTGTGGTACATTGACATGTATTTGTACAGGTTCATGTTCAAATTGTAAG
SC5.2630	**AA:** ITSISLCTPGCKTGALMGCGTLTCGCNITGGK
	DNA: ATTACTTCGATCTCATTGTGTACACCTGGTTGTAAAACAGGTGCACTTATG GGTTGTGGTACATTGACATGTGGATGCAACATCACAGGAGGTAAA
SC5.2701	**AA:** ITSISLCTPGCKSKAVCNMKKSAKHHC
	DNA: ATTACTTCGATCTCATTGTGTACACCTGGTTGTAAATCAAAAGCAGTTTGT AATATGAAAAAATCAGCTAAACATCACTGC
Peptide 1 SC5.2712	**AA:** IASKFLCTPGCATGALMGCNMKTATCNCSIHVSK
	DNA: ATTGCATCAAAATTTCTTTGTACTCCAGGTTGTGCAACAGGTGCACTTATG GGTTGTAATATGAAAACAGCTACTTGTAATTGTTCAATTCACGTTTCAAAA
SC5.2829	**AA:** ITSISLCTPGCATGALMGCNMKTATCNCSIHVSK
	DNA: ATTACTTCGATCTCATTGTGTACTCCAGGTTGTGCAACAGGTGCACTTATG GGTTGTAATATGAAAACAGCTACTTGTAATTGTTCAATTCACGTTTCAAAA
Peptide 3 SC5.2930	**AA:** IASKFLCTPGCKTGALMGCNMSTATCNCSIHVSK
	DNA: ATTGCATCAAAATTTCTTTGTACACCTGGTTGTAAAACAGGTGCACTTATG GGTTGTAATATGTCAACAGCTACTTGTAATTGTTCAATTCACGTTTCAAAA
SC5.9487	**AA:** IASKFLCTRQVCPSKAVCRLFTATCNCSIHVSK
	DNA: ATTGCATCAAAATTTCTTTGTACACGTCAAGTTTGTCCATCAAAAGCAGTT TGTCGCCTTTTTACAGCTACTTGTAATTGTTCAATTCACGTTTCAAAA
SC5.9925	**AA:** ITSISLCTLTVECSDVAGCGTLTCGCNITGGK
	DNA: ATTACTTCGATCTCATTGTGTACTTTGACAGTTGAGTGTTCTGATGTGGCT GGCTGTGGTACATTGACATGTGGATGCAACATCACAGGAGGTAAA

Supplementary References

1. Kuipers, O. P., de Ruyter, P. G. G. A., Kleerebezem, M. & de Vos, W. M. Quorum sensing-controlled gene expression in lactic acid bacteria. *Journal of biotechnology* **64**, 15-21, doi:10.1016/S0168-1656(98)00100-X (1998).
2. Kuipers, O. P., Beerthuyzen, M. M., Siezen, R. J., and De Vos, W. M. Characterization of the nisin gene cluster *nisABTCIPR* of *Lactococcus lactis*. Requirement of expression of the nisA and nisI genes for development of immunity. *European journal of biochemistry.* **216**, 281-291, doi:10.1111/j.1432-1033.1993.tb18143.x (1993).
3. Clinical and Laboratory Standards Institute. Performance standards for antimicrobial susceptibility testing; twenty-second informational supplement M100-S22. *Wayne*, PA **32**, (2013).
4. Schaefler, S., Perry, W. & Jones, D. Methicillin-resistant strains of *Staphylococcus aureus* phage type 92. *Antimicrobial agents and chemotherapy.* **15**, 74-80, doi:10.1128/aac.15.1.74 (1979).
5. Patel, R., Uhl, J. R., Kohner, P., Hopkins, M. K. & Cockerill, F. R. Multiplex PCR detection of *vanA*, *vanB*, *vanC-1*, and *vanC-2/3* genes in enterococci. *Methods in molecular medicine* **35**, 703-707, doi:10.1385/1-59259-077-2:3 (1997).
6. Lanie, J. A. et al. Genome sequence of Avery's virulent serotype 2 strain D39 of *Streptococcus pneumoniae* and comparison with that of unencapsulated laboratory strain R6. *Journal of bacteriology* **189**, 38-51, doi:10.1128/JB.01148-06 (2007).
7. Tettelin, H. et al. Complete genome sequence of a virulent isolate of *Streptococcus pneumoniae*. *Science* **293**, 498-506, doi:10.1126/science.1061217 (2001).
8. Ivanova, N. et al. Genome sequence of *Bacillus cereus* and comparative analysis with *Bacillus anthracis*. *Nature* **423**, 87-91, doi:10.1038/nature01582 (2003).
9. Hanahan, D. Techniques for transformation of *E. coli*. *DNA cloning: a practical approach* **1**, 109-135 (1985).
10. Miki, T., Ae Park, J., Nagao, K., Murayama, N. & Horiuchi, T. Control of segregation of chromosomal DNA by sex factor F in *Escherichia coli*. *Journal of molecular biology* **225**, 39-52, doi:10.1016/0022-2836(92)91024-j (1992).
11. Bernard, P. & Couturier, M. Cell killing by the F plasmid CcdB protein involves poisoning of DNA-topoisomerase II complexes. *Journal of molecular biology* **226**, 735-745, doi:10.1016/0022-2836(92)90629-x (1992).
12. Rink, R., Kuipers, A., de Boef, E., Leenhouts, K. J., Driessen, A. J., Moll, G. N. & Kuipers, O. P. Lantibiotic structures as guidelines for the design of peptides that can be modified by lantibiotic enzymes. *Biochemistry* **44**, 8873-8882, doi: 10.1021/bi050081h (2005).
13. Khosa, S., AlKhatib, Z. & Smits, S. H. J. NSR from *Streptococcus agalactiae* confers resistance against nisin and is encoded by a conserved *nsr* operon. *Biological chemistry* **394**, 1543-1549, doi:10.1515/hsz-2013-0167 (2013).
14. Khosa, S., Frieg, B., Mulnaes, D., Kleinschrodt, D., Hoeppner, A., Gohlke, H. & Smits, S.H. Structural basis of lantibiotic recognition by the nisin resistance protein from *Streptococcus agalactiae*. *Scientific reports* **6**: 18679, doi:10.1038/srep18679 (2016).
15. Bruun, T.-H., Mühlbauer, K., Benen, T., Kliche, A. & Wagner, R. A mammalian cell based FACS-panning platform for the selection of HIV-1 envelopes for vaccine development. *PLoS one* **9**: e109196, doi:10.1371/journal.pone.0109196 (2014).
16. Silva-Rocha, R. et al. The standard european vector architecture (SEVA): a coherent platform for the analysis and deployment of complex prokaryotic phenotypes. *Nucleic acids research.* **41**, D666-D675, doi:10.1093/nar/gks1119 (2013).
17. Kuipers, A., de Boef, E., Rink, R., Fekken, S., Kluskens, L. D., Driessen, A. J., Leenhouts, K., Kuipers, O. P. & Moll, G. N. NisT, the transporter of the lantibiotic nisin, can transport fully modified, dehydrated, and unmodified prenisin and fusions of the leader peptide with non-lantibiotic peptides. *Journal of biological chemistry* **279**, 22176-22182, doi:10.1074/jbc.M312789200 (2004).
18. Endy, D. Foundations for engineering biology. *Nature* **438**, 449-453 (2005).
19. Shaner, N. C., Campbell, R. E., Steinbach, P. A., Giepmans, B. N., Palmer, A. E. & Tsien, R. Y. Improved monomeric red, orange and yellow fluorescent proteins derived from *Discosoma* sp. red fluorescent protein. *Nature biotechnology* **22**, 1567-1572, doi:10.1038/nbt1037 (2004).
20. Rink, R., Wierenga, J., Kuipers, A., Kluskens, L. D., Driessen, A. J., Kuipers, O. P. & Moll, G. N. Production of dehydroamino acid-containing peptides by *Lactococcus lactis*. *Applied and environmental microbiology* **73**, 1792-1796, doi:10.1128/AEM.02350-06 (2007).
21. Montalban-Lopez, M., Deng, J., van Heel, A. J. & Kuipers, O. P. Specificity and application of the lantibiotic protease NisP. *Frontiers in microbiology* **9**: 160, doi:10.3389/fmicb.2018.00160 (2018).
22. Roberts, T. M., Rudolf, F., Meyer, A., Pellaux, R., Whitehead, E., Panke, S. & Held, M. Identification and characterisation of a pH-stable GFP. *Scientific reports* **6**: 28166, doi:0.1038/srep28166 (2016).